AMERICAN UNIVERSITY OF BEIRUT

A NUMERICAL MODELING APPROACH TO EVALUATE ENERGY-EFFICIENT MECHANICAL VENTILATION STRATEGIES

by
BILAL IBRAHIM YASSINE

A thesis
submitted in partial fulfillment of the requirements
for the degree of Master of Mechanical Engineering
to the Department of Mechanical Engineering
of the Faculty of Engineering and Architecture
at the American University of Beirut

Beirut, Lebanon
July 2012

AMERICAN UNIVERSITY OF BEIRUT

A NUMERICAL MODELING APPROACH TO EVALUATE ENERGY-EFFICIENT MECHANICAL VENTILATION STRATEGIES

by

BILAL IBRAHIM YASSINE

Approved by:

Dr. Kamel Ghali, Professor Department of Mechanical Engineering	Advisor
Dr. Nesreen Ghaddar, Professor Department of Mechanical Engineering	Member of Committee
Dr. Ghassan Chehab, Associate Professor Department of Civil Engineering	Member of Committee
Dr. Issam Srour, Assistant Professor Engineering Management Program	Member of Committee

Date of thesis defense: July 16, 2012

AMERICAN UNIVERSITY OF BEIRUT

THESIS RELEASE FORM

I, Bilal Ibrahim Yassine

☐ authorize the American University of Beirut to supply copies of my thesis to libraries or individuals upon request.

☐ do not authorize the American University of Beirut to supply copies of my thesis to libraries or individuals for a period of two years starting with the date of the thesis defense.

_____
Signature

_____
Date

ACKNOWLEDGMENTS

I would like to acknowledge my thesis advisor Prof. Kamel Ghali for all his support and assistance throughout the development of the research.

Moreover, I would like to express all my thanks to Prof. Nesreen Ghaddar, Prof. Ghassan Chehab, and Prof. Issam Srour, my thesis committee members, for all their help and cooperation in the success of the work.

I would like to acknowledge the support of Eng. Amer Keblawi for his continuous help throughout this research; without him this research would have taken much more time to be finished.

I would also like acknowledge the support and help of my friends: Sarah Kadri, Mohyeddine Al Khatib, Ahmad El Merhib, Chadi Awad and to the guy I have been spending my time, in the last two years, more than my family Mohammad Hammoud. Without their support and cooperation I would never have the power to step over the difficulties I have faced during my undergraduate and graduate studies.

Thanks to all my new friends and colleagues I have met in the last two years at AUB, whom I have shared unforgettable moments and who supported me during my research work time.

A special thanks to my brother, my sister and my sister in law if it wasn't for their support I would not have been at this place at this time.

Last but not least, I will never be able to thank enough my father and my mother for their great patience and support during my whole life. Without them I would never been the person I am.

AN ABSTRACT OF THE THESIS OF

Bilal Ibrahim Yassine for Master of Mechanical Engineering
Major: Applied Energy

Title: A Numerical Modeling Approach to Evaluate Energy-Efficient Mechanical Ventilation Strategies

This thesis investigates design features that can potentially reduce the energy consumed in attaining appropriate thermal comfort levels in typical residential buildings in urban and rural settings. A numerical model coupled with a PID controller is developed to predict the indoor air temperature that is adjusted via mechanical ventilation. The model is used to simulate and evaluate various scenarios of building wall layouts and materials. From the various simulation runs, the wall configurations and materials were refined to combinations that rendered the mechanical ventilation a feasible option for attainment of comfort for the largest number of hours per year. The runs were conducted for two typical residential apartment located in the city of Beirut, Lebanon, representative city for the urban settings, and for the Bekaa region, representative city for the rural settings. The same wall configurations were examined both settings. Different wall configurations were assumed for each of the living zone and the bedroom zone of the apartment. The simulation results suggest an optimal wall configuration comprised of a 5 cm layer of insulating strawboard sandwiched between a 2 × 10 cm wall made of masonry units consisting of Hempcrete (mixture of Portland cement, aggregates, and industrial hemp fibers) for the living zone for both location the rural and urban areas, whereas the wall for the bedroom zone in the urban setting consists of a 10 cm of Hempcrete and in the rural setting consists of a 10 cm of Hempcrete in addition to 5 cm layer of insulating strawboard.

CONTENTS

ILLUSTRATIONS

Figure Page

TABLES

Dedication addressed

To my family

CHAPTER 1

INTRODUCTION

Worldwide, the building sector accounts for 50 percent of total energy consumption (UNEP 2007). This percentage is expected to increase with population growth and climate change compounding the problem of dwindling energy resources. In an effort to minimize this increase in the building's energy demand, there is a growing movement towards the design, construction, and operation of energy efficient buildings (Kesselring and Winter 1994, Pfeiffer *et al.* 2005, Schulz *et al.* 2008) .

The majority of the research effort in this field (Tran *et al.* 2010, Kolokotroni *et al.* 1999, Blondeau *et al.* 1997, Carrilho da Graca *et al.* 2002 and Eicker 2010) has focused on methodologies, innovations, and initiatives aimed at reducing the operational energy consumption. Examples include development of energy efficient electro-mechanical systems (e.g., HVAC units, lighting), use of renewable energy, and adoption of incentives for use of building envelopes that provide high insulation and air tightness.

One means of mitigating the increase in energy consumption is by relying on mechanical ventilation systems for cooling purposes and on the applications of natural (as compared to processed and manufactured) and recycled materials in building construction. Incorporation of natural ventilation systems and ceiling fans lead to a decrease in the usage of mechanical air conditioning systems and help attain indoor air quality and thermal comfort at higher air temperatures.

Several studies have shown that mechanical ventilation contributes to energy efficient buildings especially for buildings with appropriate thermal mass and sufficient daily temperature swing from day to night. On the other hand, the use of natural material such as industrial hemp fibers mixed with concrete has been reported to have low heat conductivity in comparison with other building materials in construction; thus, it reduces the summer heat gains and winter heat losses (Tran *et al.* 2010).

Several studies have investigated the impact of ventilation on the internal indoor air temperature (Kolokotroni *et al.* 1999, Blondeau *et al.* 1997, Carrilho da Graca *et al.* 2002 and Eicker 2010). The key parameters related to the efficiency of ventilation can be divided into three categories: climatic factors, building material and control strategy parameters. An example of climatic factors is the outdoor air temperature, which includes mean daily temperature and diurnal temperature range, i.e. the climatic potential index. Building parameters include the building type, envelope openings such as windows and doors, building material and building structure. The flow rate and time period are determined by the control strategy when mechanical ventilation is applied (night ventilation, day time ventilation, full-day ventilation and no ventilation).

(Kolokotroni *et al.* 1999, Blondeau *et al.* 1997, Carrilho da Graca *et al.* 2002 and Eicker 2010) concluded that the use of night ventilation contributes to energy efficient buildings especially for buildings with appropriate thermal mass and sufficient daily temperature swing from day to night. Similarly, daytime ventilation (mechanical and natural) was determined to be applicable and energy efficient for all buildings. However, in regions that lack wind speed such as high density cities where the building's structure blocks the wind field, replenishing indoor air for occupant thermal comfort can be achieved only by mechanical ventilation (Geros *et al.* 1999, Shaviv *et al.*

2001 and Zhou *et al.* 2008). (Zhou *et al.* 2008) discussed the effect of coupling the thermal mass and natural ventilation on the passive building design. They tested different wall configurations and found that heavy walls with external insulation provide the lowest amplitude of indoor air temperature among different external low mass walls.

Nonetheless, the use of natural, mechanical or even hybrid (natural and mechanical) ventilation systems with optimized building envelop, consisting of natural building material, cannot insure thermal comfort conditions throughout the year. Additional systems would thus be necessary to aid in providing continuous thermal comfort. One such system, the Earth to Air Heat Exchanger (EAHX), has been found to have the potential of decreasing (increasing) the temperature of the air supplied to the space in summer (winter).

(Kusuda *et al.* 1965, Labs 1989 and Krarti 1995) have reported that the ground temperature differs from the ambient temperature. This is due to the fact that the temperature fluctuation at the surface of the ground diminishes as the depth of the ground increases due to the high thermal inertia of the soil. Hence, an Earth to Air Heat Exchanger system can utilize the soil as a heat source/sink to moderate the outdoor air. An EAHX consists of a buried pipe with access to open air. The performance of an EAHX depends on pipe length and diameter, air velocity, the air flow rate inside the pipe and the pipe burial depth.

Several studies (Lee and strand 2008, Mihalakakou *et al.* 1995 and Bansal *et al.* 2010) have investigated the effect of these parameters on the overall performance of the earth pipe under various conditions. It was found that during the summer (winter) as

the pipe length and depth increases, the outlet air temperature from the pipe decreases (increases). As the air flow rate increases, the EAHX outlet air temperature increases since air has less contact time through the pipe. Additionally, as the radius of the pipe increases, the outlet air temperature increases due to the resulting decrease in the heat transfer coefficient. A pipe length of 70m, located at a depth of 3m and velocity of 2m/s to be an effective configuration (Lee and strand 2008, Mihalakakou *et al.* 1995). The EAHX was found to be energy effective in providing indoor comfort in the cold climate of Europe in winter by increasing the outdoor air temperature by $5^{o}C$ and decreasing it in summer by $12.7^{o}C$ (Bansal *et al.* (2010), Jacovides and Mihalakakou 1995, Ascione *et al.* 2011 and Hollmuller and Lachal 2001). Moreover, (Ajami *et al.* 2006) have reported that an EAHX can reduce the cooling energy demand of a typical Kuwaiti house by 30%.

The EAHX option is more feasible in inland areas where houses are surrounded by adequate outdoor area in which pipes can be buried than multi-storied apartment buildings in urban areas with limited outdoor space. This lead to a reduction in building's heating and cooling needs since the outlet temperature of the earth tube in summer is lower than the outdoor air temperature while in winter it is higher. The thesis investigates the feasibility and efficiency of coupling an EAHX with a mechanical ventilation system in providing thermal comfort.

A drawback of the EAHX is the fact that it requires long piping to be buried in the soil. This increases the initial cost of the system (excavation and materials) and energy demand during operation. The high energy demand results from the high pressure required to force the needed air flow rate in the buried pipes. As the length of

the pipe increases, the frictional losses inside the pipe increase, resulting in a higher energy demand.

In terms of natural material, wood, sisal, jute, bamboo, coconut, asbestos, rockwool and hemp are examples that can be used. Along those lines, an innovative building material that has shown to yield multiple socio-economic benefits is Hempcrete. Hempcrete is a mix of cement mortar with fibers of Industrial Hemp, a sister plant of cannabis. The benefits of using hemp have been reported by a study conducted by (Awwad *et al.* 2010). The study shows that Hempcrete: (i) improves physical characteristics and structural performance of concrete; (ii) reduces raw materials and energy resources; (iii) provides a material with better thermal property and therefore increases energy efficiency. With such benefits, and being a carbon neutral material, the use of hemp in concrete reduces the embodied energy of concrete and other cementitous materials which are widely used and in large quantities in building construction.

This thesis further investigates options to lower operational energy without negatively affecting embodied the energy of typical apartments in urban and rural settings by conducting research that considers both the building materials and a hybrid mechanical ventilation system for comfort and air quality. The thesis focuses, through two case studies in the urban and rural area of Lebanon on the use of local and regional materials such as strawboard for insulation and hemp in concrete that contribute to the decrease in the building embodied and operational energy. In addition, the thesis proposes a space model for controlling the amount of ventilation air needed for conditioning the building's indoor environment. The thesis does not consider natural ventilation as there are many uncontrollable variables (blockage of urban wind by high

rise building, uncontrolled outside air velocity, security issues) which could affect its reliability as an effective air conditioning option. Mechanical ventilation and ceiling fans are used to adjust the indoor air temperature and speed whenever needed to achieve thermal comfort.

For the urban area, a typical apartment in Beirut city, Lebanon is considered as a case study. In Beirut, Direct Mechanical ventilation is used to moderate the temperature inside the space due to the space limitations. On the other hand, for the rural areas, a typical apartment in the inland region of Lebanon (Bekaa region) is considered as a case study. In Bekaa, a hybrid mechanical system is used which can draw ventilation air directly from outside or can bring it through an earth tube that is buried in soil is used to achieve thermal comfort in the space for the larger period of time during the year (Figure 1). The hybrid system has the potential of decreasing the operational energy of a residential house in urban and rural settings.

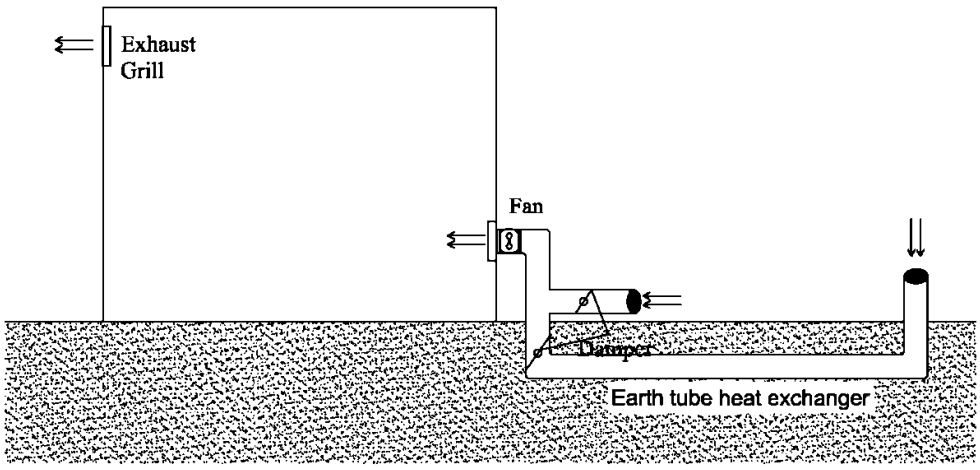

Fig. 1: Inland Region Ventilation system

Any fluctuations in outside temperature or solar load can cause the internal air temperature to fluctuate in a similar way, though delayed and dampened depending on the thermo-physical properties (thermal capacitance, resistance and density) of the building wall construction materials as well as its layering arrangement. The effectiveness of mechanical ventilation in achieving thermal comfort for a given building construction material is determined through the reliability of this system in offering thermal comfort without having the need to resort to mechanical cooling during summer and winter operations.

CHAPTER 2

SIMULATION MODELS

To meet the objective of this thesis, a mechanical ventilation controller integrated with a numerical multi-zonal space and comfort models is developed. For given building materials and a set of indoor and outdoor conditions, the ventilation controller modulates the amount of ventilation air needed to moderate the indoor air temperature and minimize discomfort hours. Different building materials are assessed for both their effect on indoor comfort and fan consumption. The numerical space model is validated against other commercial simulation software that simulates indoor air temperature for Lebanon conditions.

2.1. Space Model

The space analyzed in the case study is divided into two zones: living and bedroom. The transient one-dimensional heat conduction equation for a multilayered wall consisting of N parallel layers is given by equation (1):

$$\rho_{i,j} c_{i,j} \frac{\partial T_{i,j}(t,x)}{\partial t} = k_{i,j} \frac{\partial^2 T_{i,j}(t,x)}{\partial x^2} \quad (1)$$

where: i represents building element (wall, ceiling, or floor), j represents the j^{th} layer within the element i, t and x are the time and spatial coordinates respectively, $T_{i,j}$ is the temperature, whereas k, ρ, and c are the thermal conductivity, density, and thermal capacity respectively.

The boundary conditions for the outdoor and indoor surfaces of the wall are

$$\alpha.I(t) + h_{c\infty}[T_{\infty}(t) - T_i(0,t)] + h_{r\infty}[T_{sky}(t) - T_i(0,t)] = -k\,\frac{\partial T_{i,j}(0,t)}{\partial x} \quad (2)$$

$$h_{ca}[T_i(L,t) - T_a(t)] + \sum_{j=1}^{6} h_{ri-j}[T_i(L,t) - T_j(t)] = -k\,\frac{\partial T_i(L,t)}{\partial x} \quad (3)$$

where the external radiative coefficient, $h_{r\infty}$, is equal to $\varepsilon\sigma(T_{sky} + T_i(0,t))(T_{sky}^2 + T_i^2(0,t))$ and the internal radiative coefficient, h_{ri-j}, is equal to $\varepsilon\sigma F_{i-j}(T_i(L,t) + T_j(t))(T_i^2(L,t) + T_j^2(t))$. The coefficients h_{ca} and h_r are the convective and radiative heat transfer coefficients for the outdoor and indoor wall surfaces respectively, α is the wall surface absorptivity, and *I* is the total solar radiation on the wall side. The temperatures T_{∞}, *T(0,t)*, $T_a(t)$, *T(L, t) and* T_{sky} are the ambient air and outside wall surface temperature, room air, inner wall surface temperature, and sky temperature.

The internal lumped air node energy balance is given by

$$\rho_d V_a c_{p,a}\,\frac{\partial T_a(t)}{\partial t} = \sum_{i=1}^{6} h_{c,a}.A_i(T_i - T_a) + \dot{m}c_{p,a}(T_{a,\mathrm{sup}plied} - T_a) + \sum q_{\mathrm{int}} \quad (4)$$

where: $\rho_a, V_a, and\ c_a$ are density, volume and specific heat capacity of the room air respectively, A_i and T_i are the surface area and the temperature of the room element *i,* $\dot{m}\ and\ T_{supplied}$ are the mass flow rate and the temperature of the air supplied by the ventilation system. q_{int} is the internal heat load.

The simplified dynamic moisture for the space is shown in equation (5):

$$\rho_a V_a\,\frac{d w_a}{\partial t} = G - \dot{m}\ (w_a - w_{a,\mathrm{sup}plied}) \quad (5)$$

where G is the rate of moisture generation inside the space due to latent loads, and $w_\infty \; and \; w_a$ are the room air and supply air humidity ratios.

2.2. Thermal Comfort Model

Different thermal comfort model are discussed in several studies [15-19]. The new adaptive comfort model for ASHRAE standard 55 address thermal comfort in naturally ventilated building. In this standard the temperature range that satisfies thermal comfort of people is higher than the other conservative approaches based on the predicted mean vote method (PMV) (Fanger 1970 and Kruger 2008). However, this standard is limited to building with reachable and operable windows that is controlled by human. For this reason, in this research the Predicted Mean Vote (PMV) model Fanger 1970) is used to assess the indoor thermal comfort. The PMV represents the thermal sensation of people on a scale from -3 (cold) to + 3 (hot). The model is simple, widely used by researchers and its input requirements are direct and can be categorized as environmental (temperature, relative humidity, air velocity,) and personal (clothing insulation and metabolic rate). Thermal comfort inside the space is calculated on an hourly basis, based on the room hourly average temperature, average relative humidity and air velocity for the precedent hour. Comfort inside the space is assumed to occur when the PMV inside the space is between -1 and +1.

2.3. Controller Equation

A *PID* controller is used to modulate the ventilation air flow rate based on room temperature and indoor fresh air requirement (Dorf and Bishop 2008). Every five minutes, the controller updates the ventilation air flow rate to keep the indoor air

temperature at its summer and winter set points and to provide thermal comfort for longer periods, if possible, as indoor air temperature deviates from its set point.

Equation 6, shown below, is used in controlling the ventilation flow rate:

$$\dot{m}_{(t)} = \dot{m}_{(t-1)} + \left(\begin{array}{l} K_c \left(1 + \frac{\Delta t}{TI} + \frac{TD}{\Delta t} \right) \times \left(T_{room} - T_{set\ po\ \mathrm{int}} \right) - \left(1 + 2\frac{TD}{\Delta t} \right) \times \left(T_{room} - T_{set\ po\ \mathrm{int}} \right)_{(t-1)} \\ + \frac{TD}{\Delta t} \times \left(T_{room} - T_{set\ po\ \mathrm{int}} \right)_{(t-1)} \end{array} \right) \quad (6)$$

where Δt is the time step, K_c, TI and TD are the proportional, integrative and derivative gains parameters. These parameters are tuned to minimize the air flow rate fluctuations.

2.4. Soil And Earth To Air Heat Exchanger Model

The performance of the earth-air pipe system depends on: the ambient conditions (temperature, solar radiation, relative humidity and wind velocity), the dimensions of the pipe (length and cross sectional area), the depth at which it is buried, the material used for transporting the outdoor air, the temperature of soil in the vicinity of the buried pipe, soil characteristics, and the air flow rate. The temperature of the heat sink is very important for determining the amount of heat that can be given up by air as it travels inside the pipe. (Labs 1979) developed a model to determine the temperature of the soil at any depth and time as a function of the mean ground temperature and the amplitude of the soil surface temperature variation. The model is described in depth by (Lee *et al.* 2008). According to (Labs 1979 and Krarti *et al.* 1995) the temperature of the soil at any depth z and time t can be estimated by using equation (7).

$$T_{z,t} = T_m - A_s \exp\left[-z\left(\frac{\Pi}{365\alpha_s}\right)^{0.5} \cos\left\{\frac{2\Pi}{365}\left[t - t_0 - \frac{z}{2}\left(\frac{365}{\Pi\alpha_s}\right)^{0.5}\right]\right\}\right] \quad (7)$$

where T_m, A_s, z and α_s are the mean annual ground surface temperature and amplitude, soil depth and thermal diffusivity. t and t_0 are the time and the phase constant of air.

Once the soil temperature in the vicinity of the tube is determined, the simple 1-D model of (Derbel *et al.* 2010) is used to determine the air pipe outlet temperature.

$$T_{out} = T_{amb} - [T_{amb} - T_{z,t}](1 - e^{-\sigma L}) \quad (8)$$

Where T_{out} is the temperature at the outlet of the earth tube vicinity, T_{amb} is the ambient air temperature, $T_{z,t}$ is the calculated soil temperature at a certain depth z, $(1 - e^{-\sigma L})$ represents the heat removal factor, and σ is the ratio of the overall heat transfer coefficient over the ventilation mass flow rate.

The nomenclature used in this section is shown below

A	*Area of the wall (m^2)*
C_p	*Specific heat (J/Kg.K)*
COP	*Coefficient of performance*
G	*rate of moisture generation inside the space*
h	*Heat convection coefficient ($W/m^2.K$)*
I	Total solar radiation
k	*Thermal Conductivity (W/m.K)*
K_c	*Proportional gain parameters*
$\dot{m}$	*Mass Flow Rate*
T	*Temperature in (K)*
T_m	*Average Soil Temperature (K)*
TI	*Integrative gain parameter*

TD	*Derivative gain parameter*
T	*Time (s)*
q_{int}	*Internal Heat Load*
V	*Volume of the space (m^3)*
W	*Humidity Ratio (kg H_2O / kg dry air*
X	*Axial direction*
Z	*Depth (m)*

Greek Letters

α	Thermal Diffusivity
ρ	Density
ε	wall surface absorptivity

Subscripts

a	Air
s	Soil
W	Wall
∞	Ambient

CHAPTER 3

NUMERICAL SIMULATION METHODOLOGY

As mentioned earlier, the space and comfort models are integrated with the ventilation controller model into one transient model. The model is capable of determining the amount of ventilation air that can possibly provide indoor thermal comfort for longer periods and prevent large deviations of indoor air temperature from its set point during summer and winter operations. The transient model is simulated to obtain the indoor zone thermal comfort when subjected to variable external and internal loads. This requires the following information: the space dimensions, characteristics of the construction materials, outdoor weather conditions, external and internal loads and the ventilation controller operation conditions (e.g. activation and deactivation modes). Equation (1) is solved numerically using the finite difference method with a fully implicit scheme where each wall layer is decomposed into a number of volumes, each having one node. The total number of nodes used in each wall layer is 120 nodes.

Starting from arbitrary initial conditions, and using a time step of 2.5 minutes, the inner surface temperatures of the space walls are computed along with the inner air temperature. This time step represents a compromise between accuracy and simulation runtime. Simulations are performed for typical weather conditions of each month to obtain the effectiveness of the mechanical ventilation system in providing thermal comfort throughout the entire day. At the end of the 24 hour operational period of each month, the initial conditions are recalculated and used as input in the cyclic simulations until steady periodic convergence is achieved. The criterion for convergence is reached

when the maximum percentage error for air temperature between the simulation values at time t and t + 24 hours is less than 10^{-4} percent.

3.1. Control Strategy

The strategy that is used to condition the indoor environment relies on controlling the amount of air brought to the space during summer and winter operation. The outdoor air is allowed to vary between a minimum and an upper limit. The minimum limit is determined by the fresh air requirement of 7.5 l/s/person (recommended by ASHRAE), whereas the upper limit is set to 25 ACH which is close to what has been reported by (Geroes *et al.* 1999 and Geroes *et al.* 1999) as the maximum effective rate of air change for an hour. The controller varies the amount of fresh air between the two limits to maintain an indoor temperature close to the winter and summer set points whenever the outdoor conditions allow. Otherwise, the controller prevents large deviations between indoor and outdoor temperatures. The control strategy depends on different parameters such as: the type of zone (living or bedroom), the time (day or night) and the season (winter or summer).

For the living zone, the control is active during the day (after 8 in the morning) and remains active till hour 23. During non-occupancy period (23 to 8), in the summer season, night purging with constant air flow is applied into the space; the supplied outdoor air flow takes advantage of the low temperature profile during night time throughout the summer season and helps purging the internal loads accumulated in the space during the day, while in winter the minimal requirement are applied to the space. Different values for night purging have been used in the literature (Kolokotroni *et al.* 1999 , Eicker 2010, Geroes *et al.* 1999). During summer season, an air change per

hour of 5 ACH, is close to what has been used in the Middle East region (Geroes *et al.* 1999) and close to what has been reported by (Kolokotroni *et al.* 1999 and Blondeau *et al.* 1997) and is therefore used in this thesis. As for the bedroom zone, the control is active during the occupancy time (23 till 10).

The season is a main parameter in the controller strategy; thus, the following strategy is used during the activation time period: for the winter period (November through March), the controller is set to activate whenever the indoor air temperature is lower than the outdoor ambient temperature, provided that it is lower than the winter set point temperature of 22°C, ($T_{room}<T_{amb}$ & $T_{room}<T_{setpoint}$). On the other hand, during the summer period (April through October), if the indoor air temperature is lower than the outdoor ambient temperature ($T_{room}<T_{amb}$), the amount of fresh air entering the space is set to the minimum amount of fresh air requirement recommended by ASHRAE is allowed to enter. The controller is activated whenever the indoor air temperature is higher than the outdoor ambient temperature ($T_{room}>T_{amb}$) provided that the indoor air temperature is higher than the set point temperature of 26°C ($T_{room}>T_{setpoint}$). If thermal comfort is not attained, a ceiling fan is turned on concurrently to increase the indoor air velocity to 1.5 m/s.

In the inland region, the Earth tube heat exchanger is utilized only in the living zone, during the occupancy period, the controller decides whether to use EAHX or direct ventilation system. The EAHX is utilized whenever the indoor air temperatures becomes higher than 30^{o}C in summer, or lower than 16 ^{o}C in winter, provided that it can moderate the air temperature being less than the outdoor temperature in summer and higher in winter. The earth tube is activated at 30^{o}C since discomfort inside the space

occurs at 30^{o}C with a clothing factor of 0.5, while in winter discomfort occurs when the indoor air temperature becomes lower than 16 ^{o}C with a clothing factor of 1.5 clo.

The EAHX remains active till the outdoor air temperature becomes lower than the indoor air temperature in summer (higher than the indoor air temperature in winter) or when the outdoor air temperature becomes equal to the set point; in these cases the direct ventilation system is applied.

In order to minimize the fluctuation resulting from consecutive activation and deactivation of the controller, the air temperature and the mass flow rate at time (t) are compared to those at time (t-1). If the difference is less than 5% for one of the two parameters, then the same mass flow rate at time (t-1) is used at time (t) and the indoor air temperature is simulated for this amount of air flow. Figure 2 and 3 present the flow chart of the proposed numerical model for both urban and rural areas respectively.

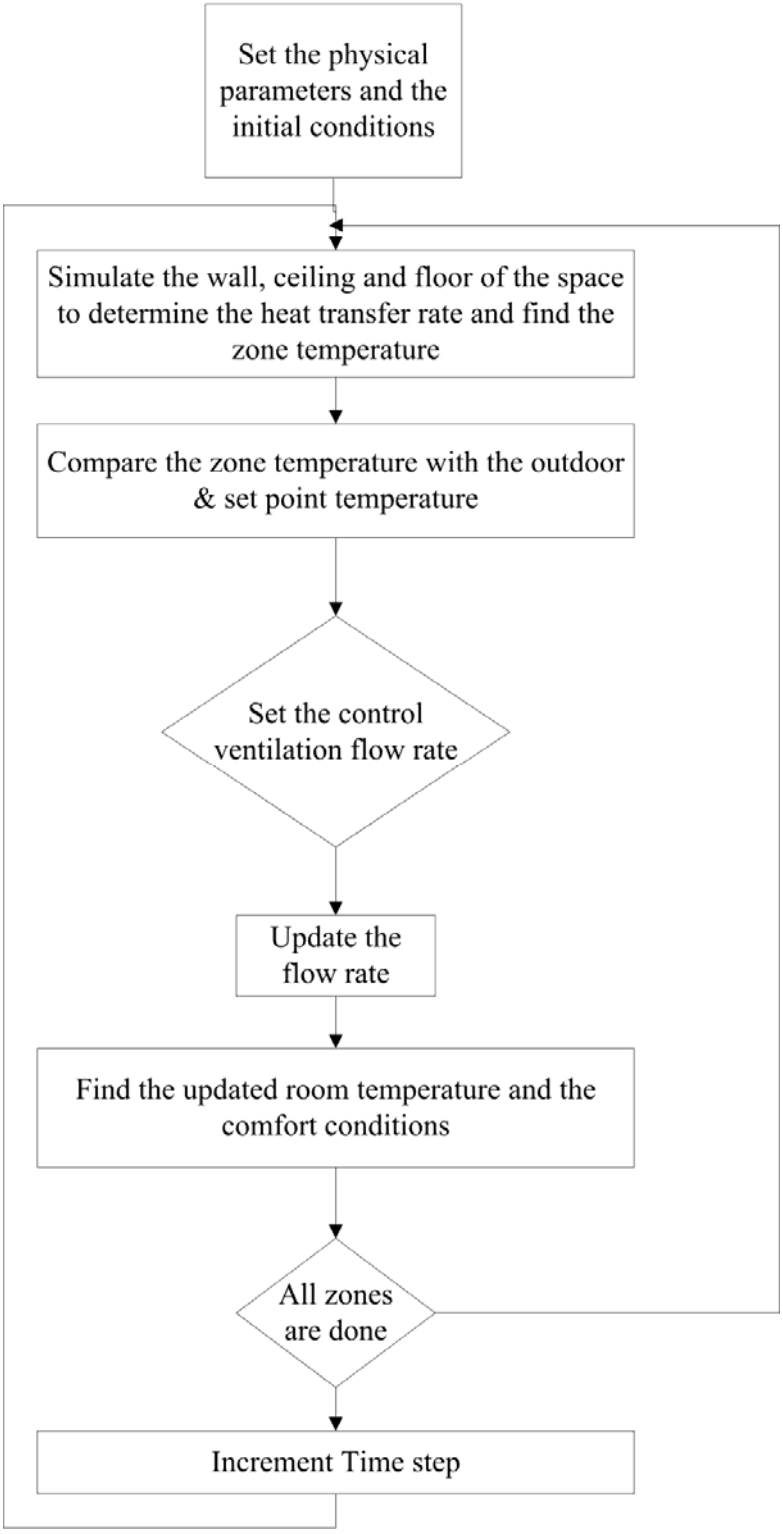

Fig. 2: Numerical model flow chart (urban setting)

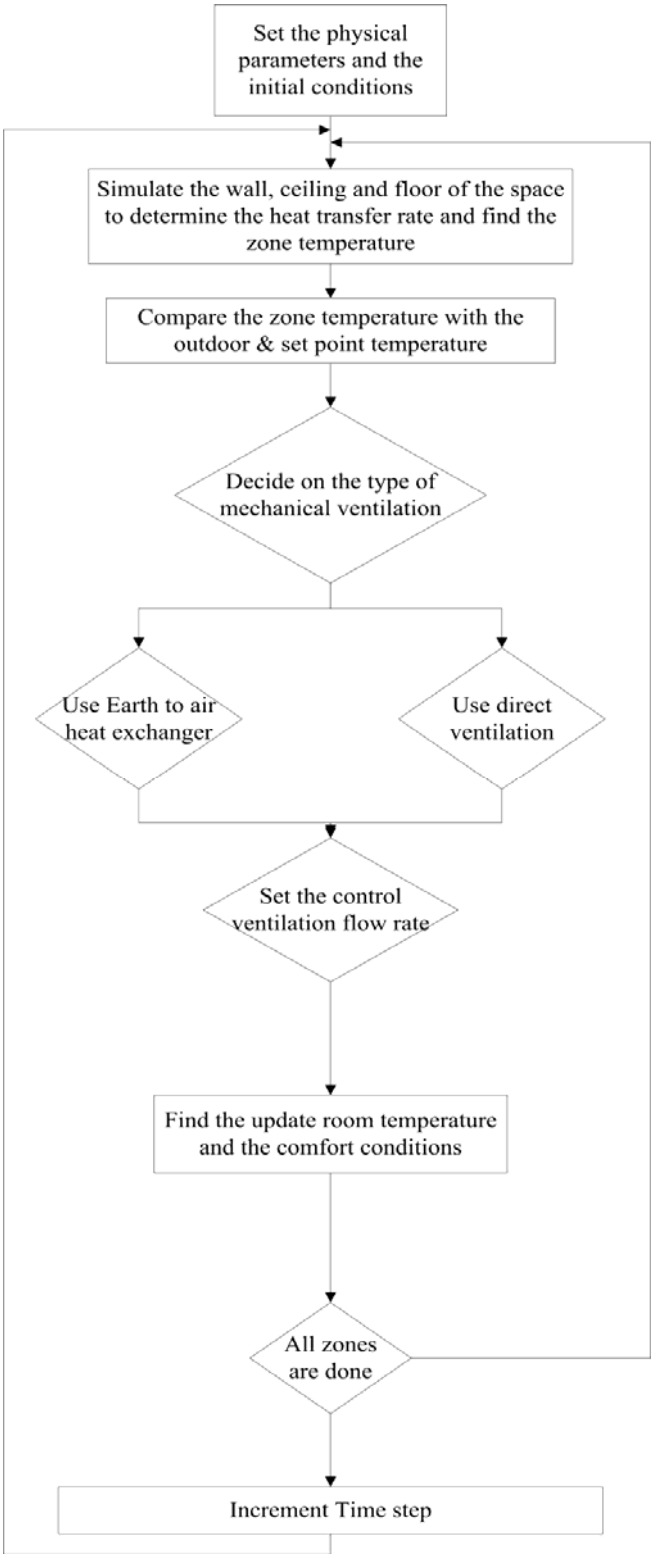

Fig. 3: Numerical model flow chart (rural setting)

CHAPTER 4

VALIDATION OF THE NUMERICAL MODEL

To ensure that the results of the numerical model are realistic and represent the real conditions of a typical residential apartment in Beirut, Lebanon, the numerical model should be validated against calibrated software such as TRNSYS which is known for its flexibility in modeling mechanical ventilation (TRNSYS 2006). This requires making sure that the results of the numerical model are accurate and also simulate the actual conditions of residential apartments in Beirut. Therefore, TRNSYS was first calibrated and then used to validate the numerical space model (TRNSYS 2006). To calibrate TRNSYS, a typical apartment in Beirut (Base case) is simulated, and the results are compared against published data on energy consumption for a typical residential apartment in Lebanon city by (Houri and Orfali 20005 and Karaki *et al.*2005). This is done by entering the data of a typical residential house in Beirut, including building structural data, operational and occupancy schedule, internal loads and outdoor climatic conditions.

Once calibrated, results from TRNSYS can serve as a benchmark to validate the results obtained from the numerical model, in a two-step process. The first step is to run the simulation software, resulting in 181 values (180 values during occupancy period (15 hours) in addition to a constant flow rate during non-occupancy (8 hours)). These values are then input from the numerical model into TRNSYS. The second step is to compare the simulated indoor air temperature provided by the numerical model to that provided by TRNSYS. The following sections elaborate on the validation effort.

4.1. Base case Description

As mentioned earlier, a typical apartment in Beirut is considered as a base case in this thesis. The apartment is assumed to have a 16 m × 10 m square layout and a height of 3 m as shown in Figure 4. It is divided into two zones: living zone (dining and living rooms) and bedroom zone (three bed rooms). The living zone has an area of 100 m^2 while the bedroom zone has an area of 60 m^2. The zones have a common partition wall and 3 external walls each. The external walls are made of 15 cm concrete masonry blocks with 1.5 cm lay mortar cement plaster on the internal and external sides of the wall, while the internal partition wall is only 10 cm thick. The external walls have an overall heat transfer coefficient of 2.36 $W/m^2 \cdot K$ and a heat capacity of 1200 J/kg and the internal partition has an overall heat transfer coefficient of 3.63 $W/m^2 \cdot K$, which is typical for urban residential apartments in Lebanon (Ministry of public works and transport 2005 and UNDP 2012) . The living zone has three external walls oriented to the North, South and West direction with an area of 30 m^2, while the bedroom has two external walls of 18m^2 area oriented the North and South, and a 30 m^2 wall oriented to the East.

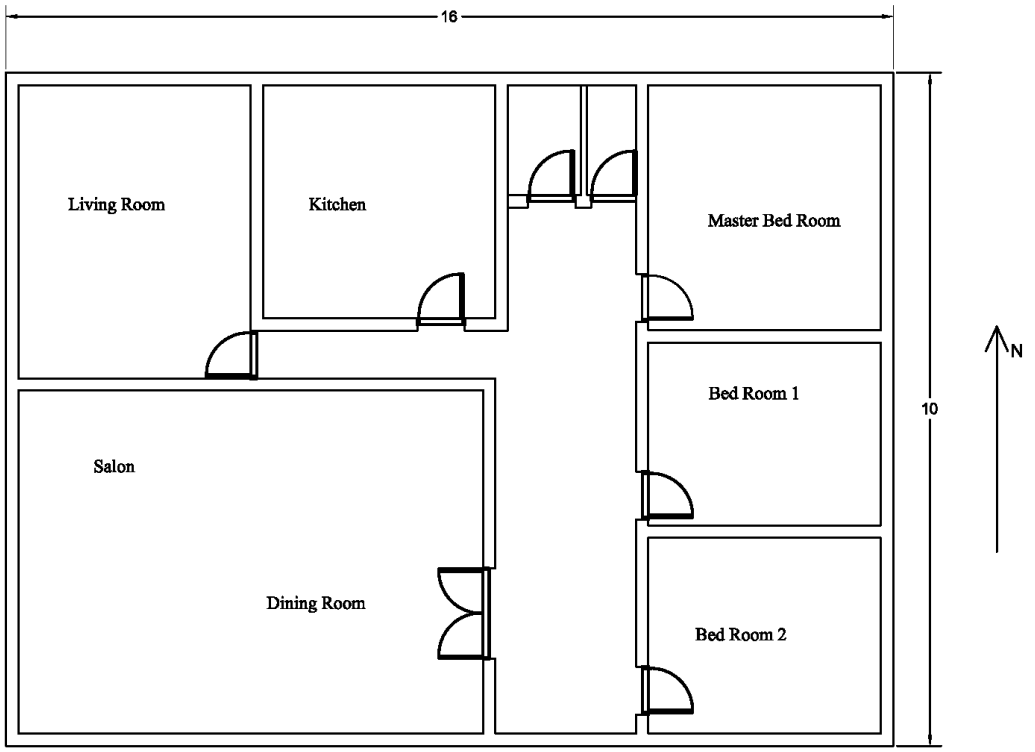

Figure 4: Typical apartment plan

The internal load component is based on the occupancy schedule of a typical Lebanese family consisting of 6 persons (Ministry of public works and transport 2005). Figure 5 shows the hourly variation in occupancy between the two zones. The electrical loads are 10 W/m^2 of sensible load for lighting fixtures and 800 W for appliances (Refrigerator, TV and PC). Figure 6 presents the schedule of the electrical load in both the living and bedroom zones. The schedule is assumed to apply for the whole year.

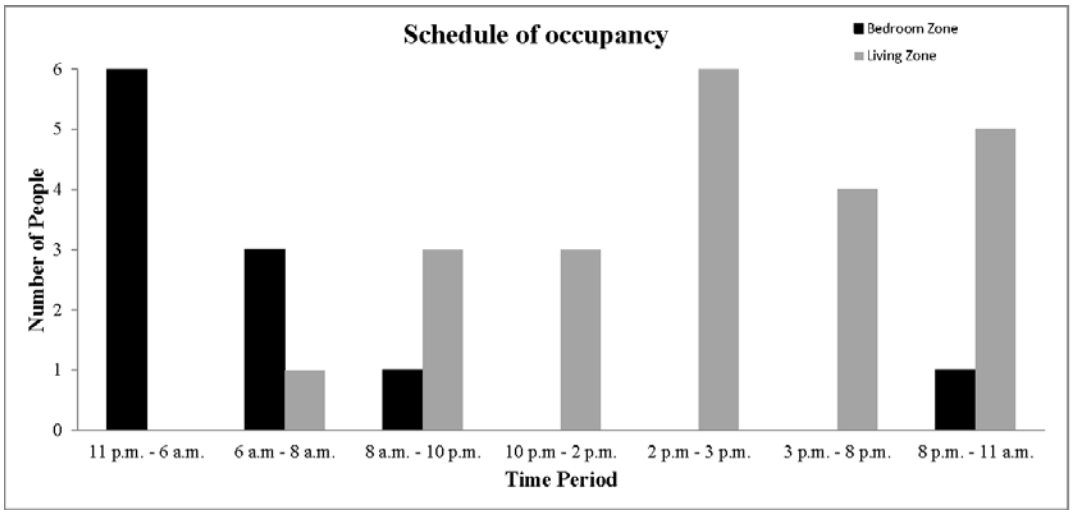

Fig. 5: Occupancy schedule inside the apartment

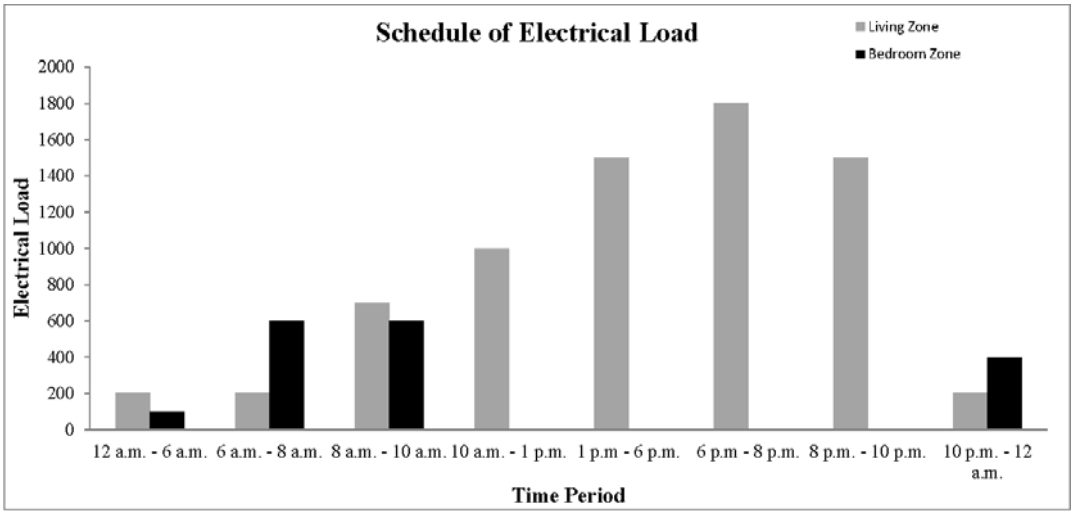

Fig. 6: Electrical load Schedule inside the apartment

4.2. Base case Calibration

A simulation of the base case using (TRNSYS 2006) showed a peak cooling load of 14.05 kW occurring at hour 16 on July 28th, with an annual cooling requirement of 132.8 kWh/m^2, and a heating peak load of 5.49 kW occurring at hour 6 in the

morning on February 12th with an annual heating requirement equal to 27.8 kWh/m^2. The weather data (outdoor air temperature, solar radiation and the relative humidity) is obtained from the records of the Mechanical Engineering Department at the American university of Beirut.

The simulations are made on an intermittent basis. During summer season, the cooling mode is activated and the heating mode is switched off; however, the system is scheduled to turn off when the temperature inside the space is lower than the set point temperature (24°C). On the other hand, during the winter season, the heating mode is activated and the cooling mode is switched off when the temperature is higher than the set point temperature (22°C). The total base case heating and cooling needs during the whole year are equal to 160.60 kWh/m^2/year of thermal energy. Using a typical energy performance of a split unit HVAC system at an average COP of 3.0, the total annual electric energy consumption of the cooling and heating system in the base case is equal to 53.53 kWh/m^2.

The total electrical energy consumption of the base case is compared against published data on the electrical energy consumption of a residential house with similar dimensions in Beirut. (Karaki *et al.*2005) reported that HVAC systems consume 50% of the total electrical energy consumption in residential houses in Lebanon at an approximate consumption rate of 48 kWh/m^2 (Houri and Orfali 2005) which is 10% different than the yearly energy consumption calculated by (TRNSYS 2006). Figure 7 shows the monthly energy consumption calculated by TRNSYS versus the results documented by (Ghaddar and Bsat 1998). A maximum deviation of 10% is found between the published and the TRNSYS simulated monthly data.

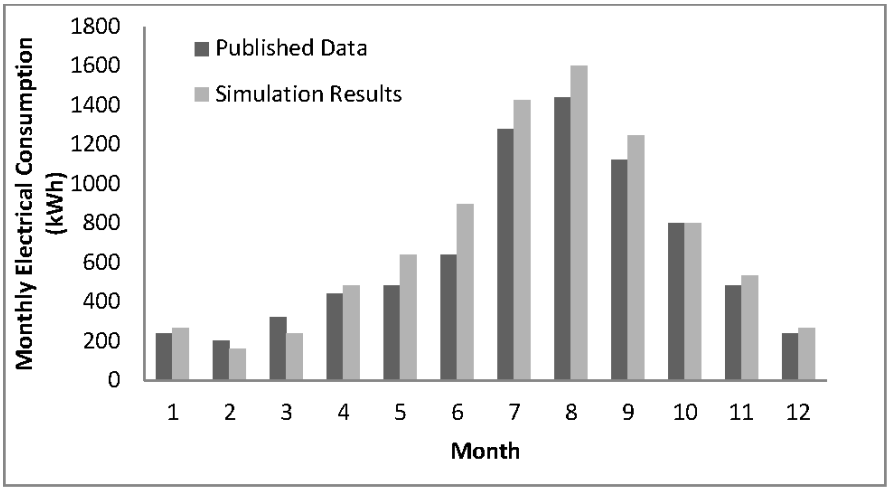

Fig. 7: Reported and simulated monthly electrical consumption of HVAC system

4.3. Comparison against TRNSYS

In order to make sure that the proposed numerical model is yielding accurate results for the zone conditions, the model is run for the living zone on August 21st and November 21st. The simulation results of the ventilation airflow rates of the numerical model are used as input in the simulation of TRNSYS to compare the resulting indoor air temperature of the numerical model and TRYNSYS. Figure 8 (a-b) shows that the space temperature, predicted by the two models, is comparable with a difference of ± 4%.

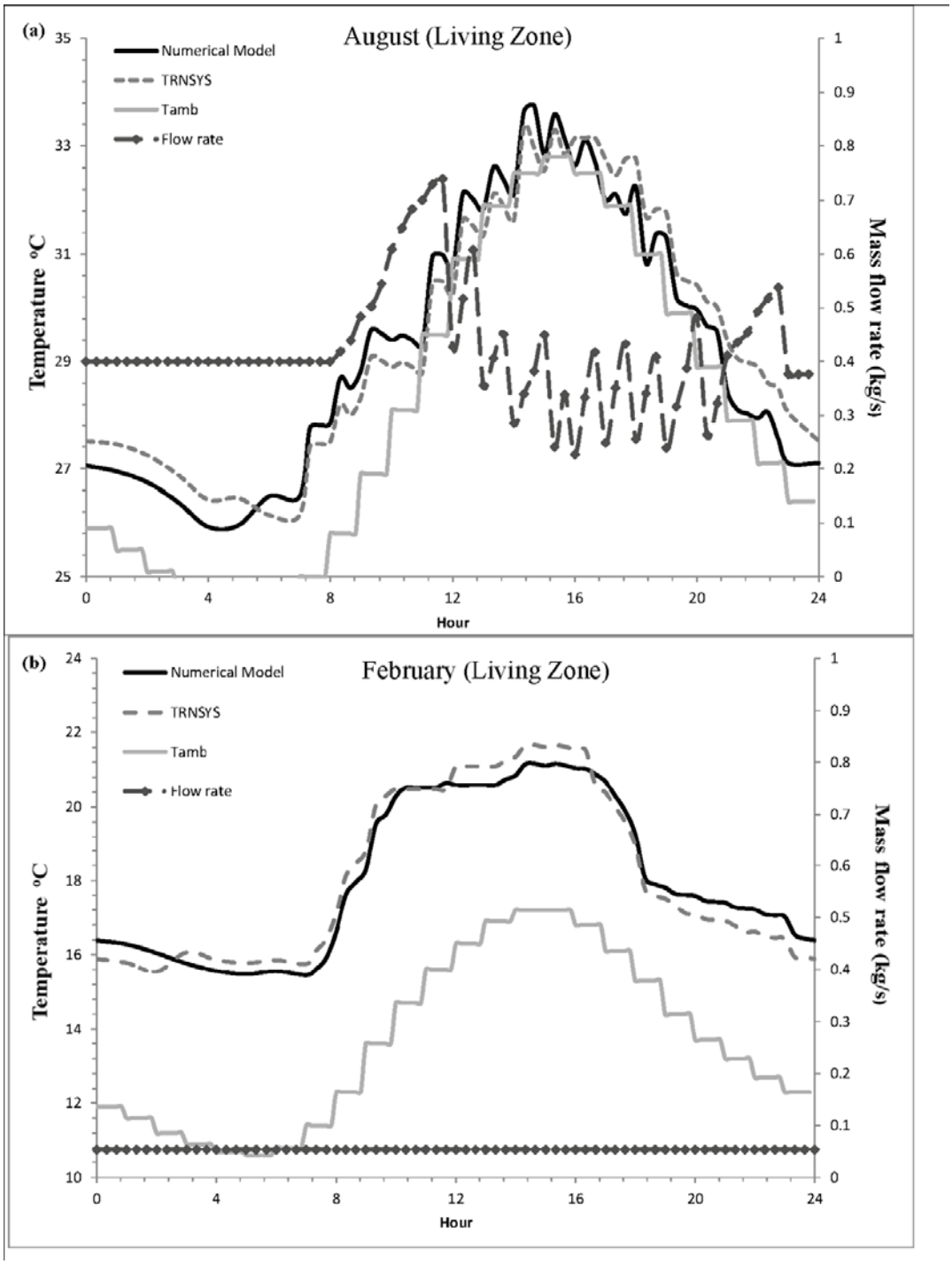

Fig. 8: Comparison between the Numerical Model and TRNSYS software of the temperature and air mass flow rate in the living zone for the months of (a) August, and (b) February.

In case of inland region, prior of determining the outlet air temperature of the soil, the soil characteristics of the inland have to be determined. (The soil map of Lebanon 2006) presents the soil physical and chemical characteristics as well as the soil texture for several locations in Lebanon. The soil texture leads to determining the soil thermal proprieties. Soil in the inland region was classified as sandy clay loam with the following thermal characteristics α_s=0.316 x10-6 m^2/s, thermal conductivity=0.503 w/m.k and heat capacity of 1.59 x103 kJ/ m^3.k.

However, in this thesis, the tube is assumed to be placed at a depth of 3 m, an air velocity of 2 m/s inside the tube is used (Lee *et al.* 2008). However, since the numerical model determines the amount of flow rate to be brought to the space, the diameter of the tube is determined based on the maximum flow rate of 1 kg/s is has been required in case of mechanical ventilation resulting in a diameter of 0.76 m. The length of the pipe that reduces the comfort hour during the month of a typical day in the summer season is taken to be the length of the pipe.

CHAPTER 5

SIMULATION RESULTS AND DISCUSSION

As mentioned earlier, the base case apartment shown in Figure 4, which is divided into two zones (living and bedroom zones), is considered as a test case for the proposed integrated space, thermal comfort, and ventilation control model. Simulations are carried out for a representative day, i.e. the 21st of each month of the year, for the city of Beirut, Lebanon. In order to obtain accurate results independent of the initial conditions, simulations are performed for 3 consecutive days, and the data for the third day are adopted in the analysis described in the following section.

5.1. Alternative Cases

To attain the objective of identifying building materials and configurations which may optimize a building energy requirements, two configurations, in addition to the base case, were examined for each of the living and bedroom zones resulting in seventy-two simulations (six simulations for each month). Several wall configurations of different building materials and wall thickness are considered for the two zones, living and bedroom. In both zones, Hempcrete is used as an alternative for the conventional concrete mix used for the masonry blocks. Hempcrete has lower thermal conductivity and higher thermal capacitance compared with the conventional hollow concrete block, and a lower embodied energy (Awwad *et al.* 2010).

The investigated configurations focus on selecting building materials that result in high insulation and capacitance in the living room zone, and low insulation and capacitance in the bedroom zone. Two wall configurations were considered for the

living zone. Case 1 consists of 3 cm of straw (C_p=2000 J/kg·K) sandwiched between 2 X 6 cm of Hempcrete (C_p=1430 J/kg·K). Case 2 (massive case) consists of 5 cm of straw sandwiched between 2 × 10 cm of Hempcrete. Two additional configurations (Case 3 and Case 4) were considered for the bedroom wall. Case 3 consists of 10 cm of Hempcrete, and Case 4 is made of 10 cm of Hempcrete and 5 cm of straw board placed on the internal side. The thermal properties of straw were obtained from "*the green building bible*" and the thermal properties of hemp were obtained from (Elfordy *et al.* 2008). Table 1 summarizes the various investigated configurations.

Table 1: Different examined scenarios of wall configuration of living and bedroom zones

Zone	Scenario	Wall configuration	U Value ($W/m^2 \cdot K$)
Both Zone	Base Case	15 cm Hollow concrete	2.36
Living Zone	Case 1	3 cm of straw sandwiched between 2 × 6 cm of Hempcrete	1.37
	Case 2 (Massive Case)	5 cm of straw sandwiched between 2 × 10 cm of Hempcrete	0.7
Bedroom Zone	Case 3	10 cm of Hempcrete	3.1
	Case 4	10 cm of Hempcrete + 5 cm of Straw	0.986

5.2. Results for the urban area

Figures 9 to 14 present the indoor air temperature for the different wall configurations, for the months of (a) February, (b) April and (c) August, representative months for the winter, spring and summer seasons. The fan power consumption is calculated based on the affinity law for prime movers. The fan power is proportional to the cube of the flow rate ratio taken with respect to a reference.

During the month of February, the mechanical ventilation controller is set to the deactivation mode for both zones (living and bedroom) since the indoor air temperature is lower than the set winter temperature and higher than the outdoor air temperature throughout the whole simulation day resulting in a fan consumption of 0.96 kWh for all the cases. For the living zone indoor temperature shown in Fig. 9(a-c), the base case wall configuration (Fig. 9(a)) characterized by lower thermal capacitance showed an indoor air temperature profile that respond to the outdoor temperature variations much more than the wall configurations for Case 1 (Fig. 9(b)) and Case 2 (massive wall, Fig. 9(c)). The thermal characteristics of the wall base case resulted in having a total of 7 discomfort hours as compared to 6 discomfort hours for Case 1 and 3 discomfort hours for Case 2. The temperature inside the living zone of Case 2, shown in Fig. 9(c), tends to be constant during the non-occupancy period, and increases slightly during the occupied time.

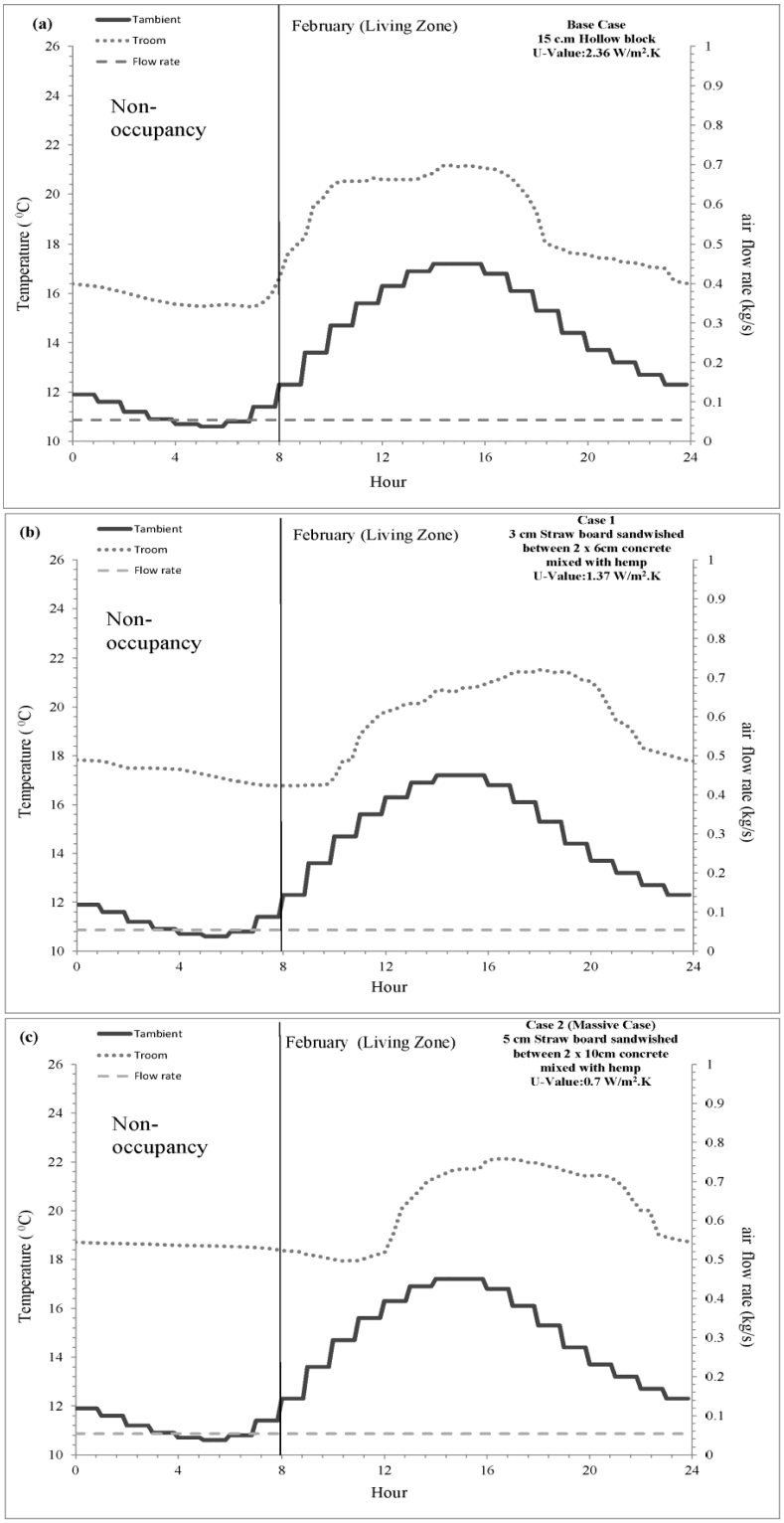

Fig. 9: Temperature and mass flow rate in the living zone during February for (a) base case, (b) Case 1, and (c) Case 2 (massive case).

As for the bedroom zone, simulations during the month of February indicate that the wall with lowest insulation (Case 3) corresponds to the lowest air temperature as shown in Fig. 10(b). This is due to a higher amount of heat loss between the indoor and the outdoor spaces. The wall with the highest insulation (U = 0.98 W/m^2·K, $C_{p,straw}$ = 2000 J/kg·K, Case 4) seems to have better conditions in the winter season since it has a higher indoor air temperature as can be seen in Fig. 10(c) and lower number of discomfort hours. Case 4 has five discomfort hours occurring during the hour period 5 till 10 compared to six and seven discomfort hours for the base case and Case 3 respectively.

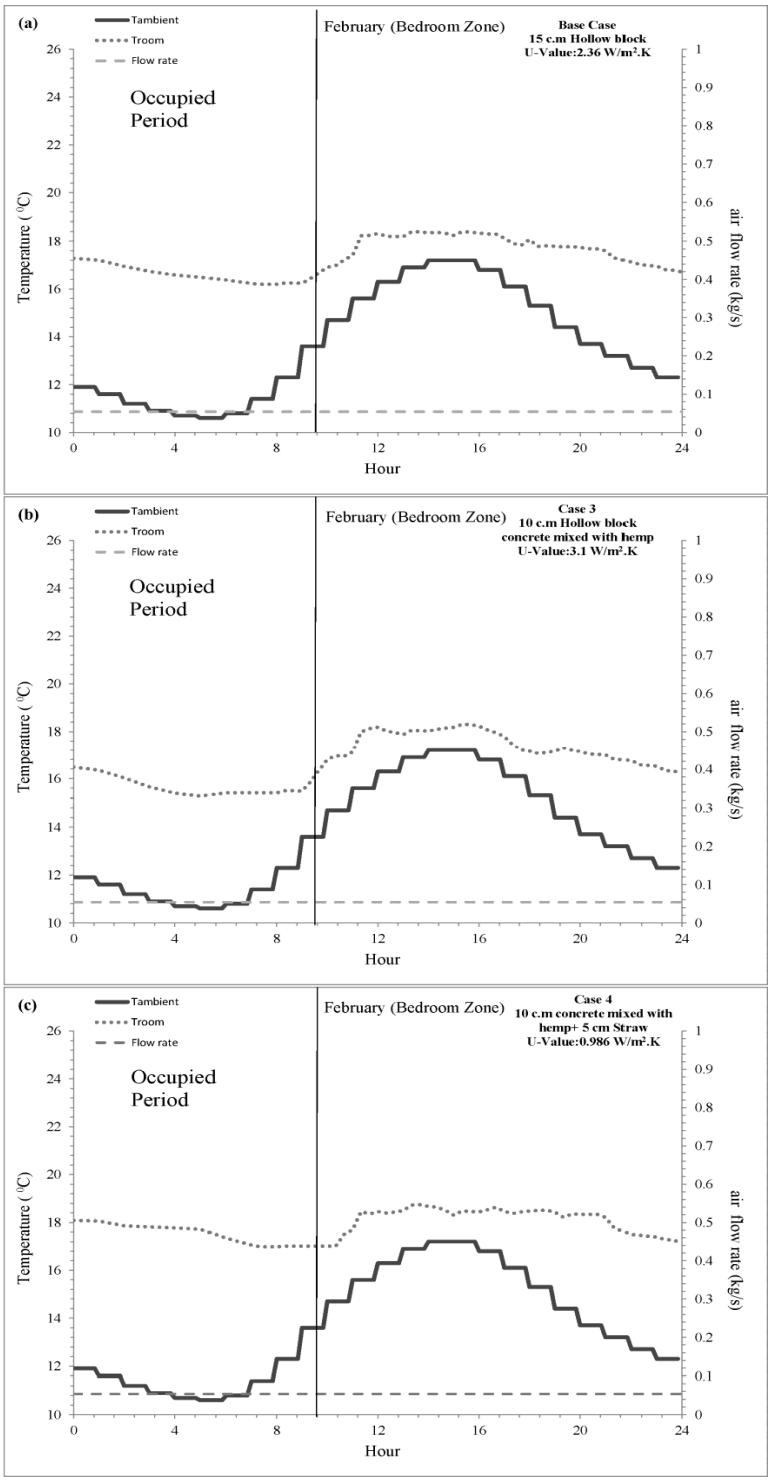

Fig. 10: Temperature and mass flow rate inside the bedroom zone during February for (a) base case, (b) Case 3, and (c) Case 4.

In the month of April (Fig. 11), night purging is applied in the living zone, and since the temperature inside the space during the occupied period is less than the set temperature, the controller is set to the deactivation mode resulting in a fan consumption of 3.32 kWh in the three cases. Both the base case and Case 1 showed an indoor living zone temperature higher than the outdoor air temperature with a general lower indoor air temperature profile for the base case (Fig. 11 a-b). As for the massive wall configuration (Case 2), the high capacitance of the wall results in having an indoor air temperature that is lower than the outdoor during the hour period of 8-15 and higher than the outdoor for the rest of the occupied period (see Fig. 11(c)).

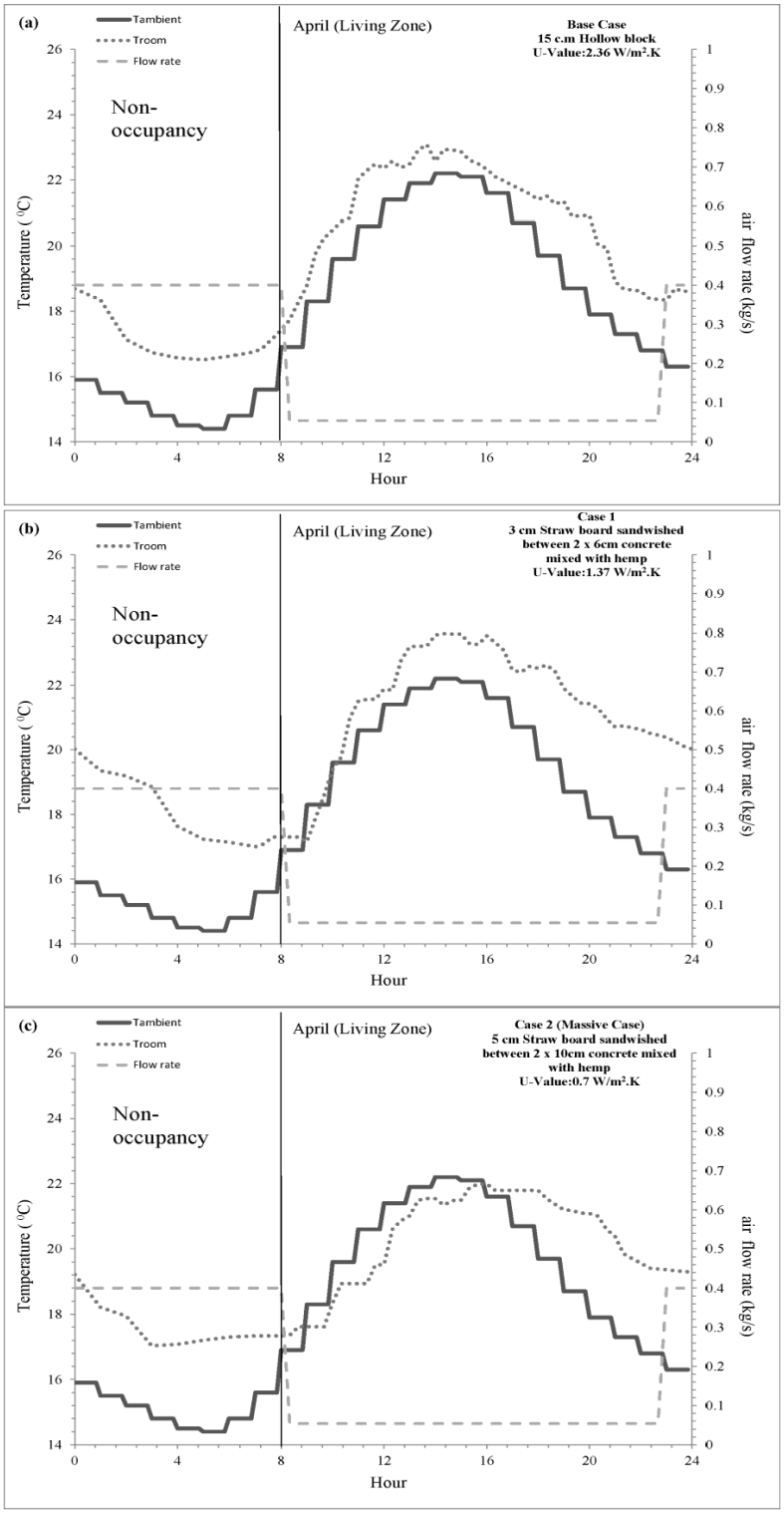

Fig. 11: Temperature and mass flow rate in the living zone during April for (a) base case, (b) Case 1, and (c) Case 2 (massive case).

In the bedroom zone (Fig. 12), the control was also set to the deactivation mode during the occupancy time, resulting in a fan consumption of 0.96 kWh. The wall case of the highest insulation (Case 4) has the highest air temperature profile, and due to its highest thermal capacitance, the temperature inside the space takes more time to increase during the non-occupied period (see Fig. 12(c)). Case 3, which is characterized by the lowest insulation, had the lowest temperature profile (see Fig. 12(b)). No discomfort hours were recorded in the different cases for both the living and bedroom zones.

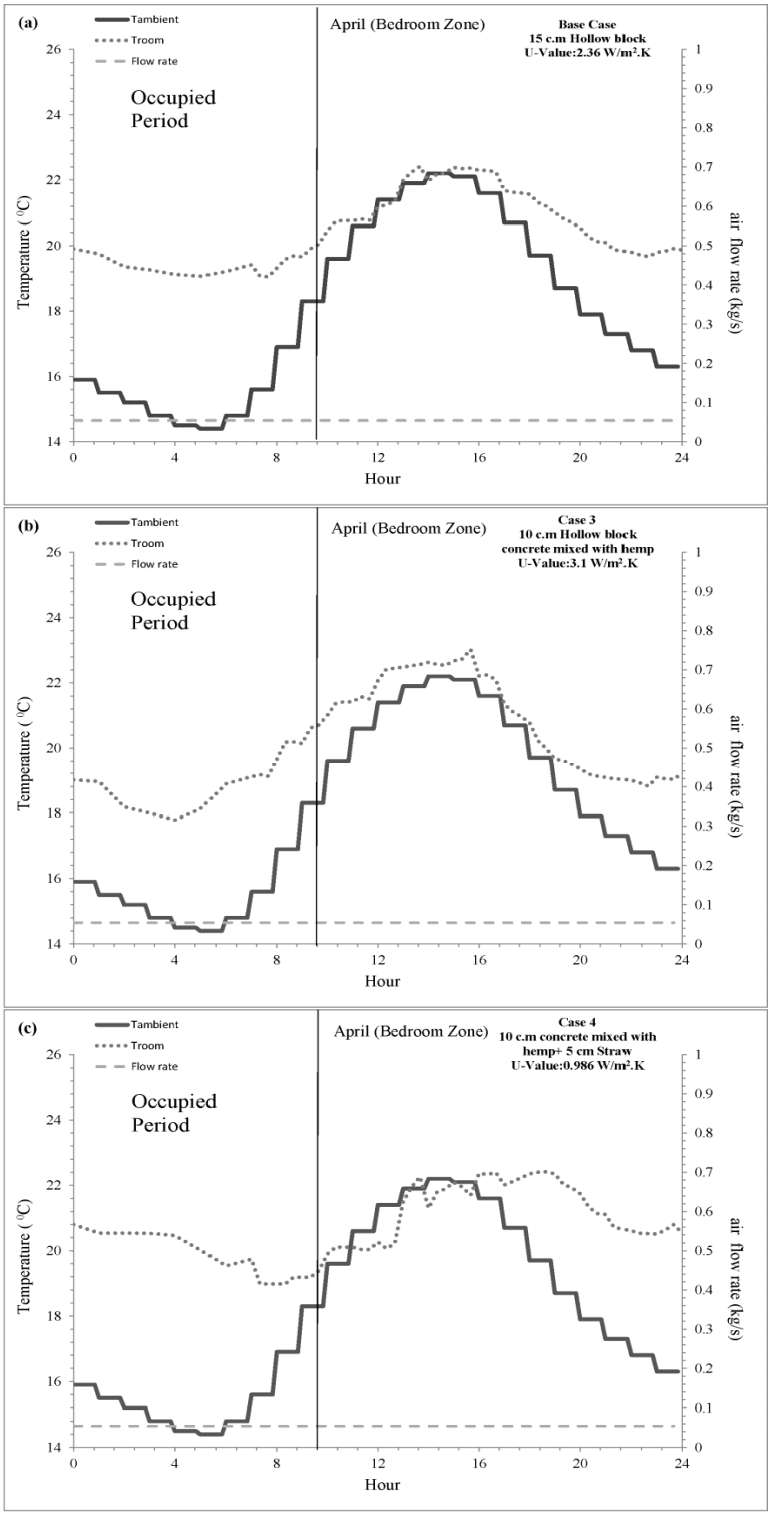

Fig. 12: Temperature and mass flow rate inside the bedroom zone during April for (a) base case, (b) Case 3, and (c) Case 4.

In August, the controller modulated the outdoor ventilation air flow to prevent the indoor air temperature from increasing beyond the outdoor air temperature for both wall configuration, Case 1 and Case 2. Figure 13(b) and (c) showed a lower indoor air temperature than in the base case shown in Fig. 13(a). However, since comfort cannot be achieved at the indoor air temperature, the ceiling fan was turned on to improve comfort conditions inside the space for the period hour extending from 12-20 and to limit the discomfort hours to seven during the hour period of 13-20 in comparison to 12 and 11 discomfort hours for the base case and Case 1 respectively.

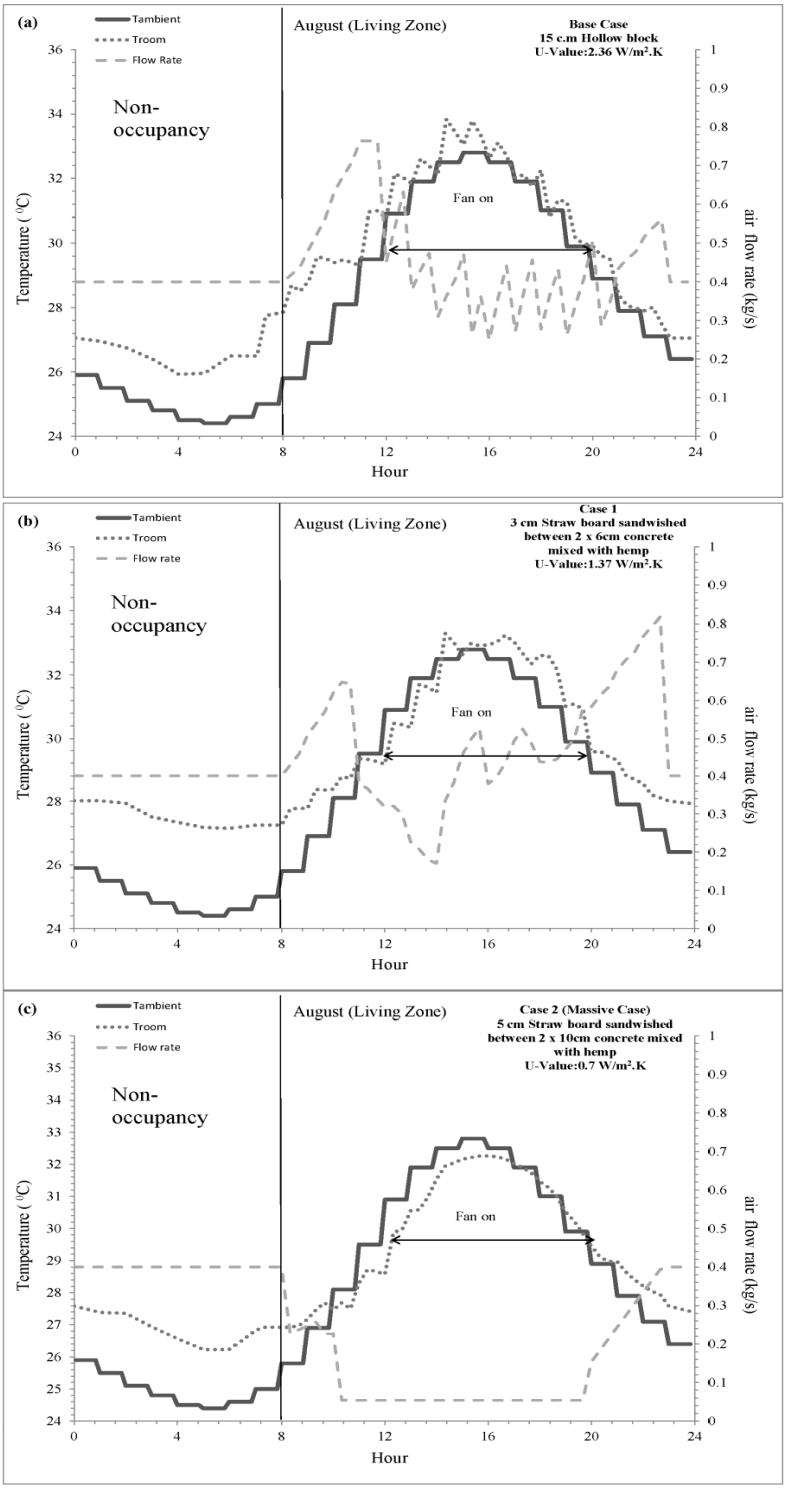

Fig. 13: Temperature and mass flow rate in the living zone during August for (a) base case, (b) Case 1, and (c) Case 2 (massive case).

In the bedroom zone, Case 3 (Fig. 14(b)), which is characterized by the highest heat transfer coefficient, had the lowest indoor air temperature at the early hours of the occupied period as compared to the bedroom air temperature of the base case (Fig. 14(a)) and Case 4 (Fig. 14(c)). Two hours of discomfort Thermal comfort was attained inside the space during occupancy with zero discomfort hours for Case 3 against two hours of discomfort for the two other bedroom wall cases (base case and Case 4), moreover due to the lower wall insulation of Case 3, less ventilation air is needed to moderate the indoor zone temperature (5.70 kWh) as compared to the base case (7.65 kWh) and (9.39 kWh) for wall Case 4.

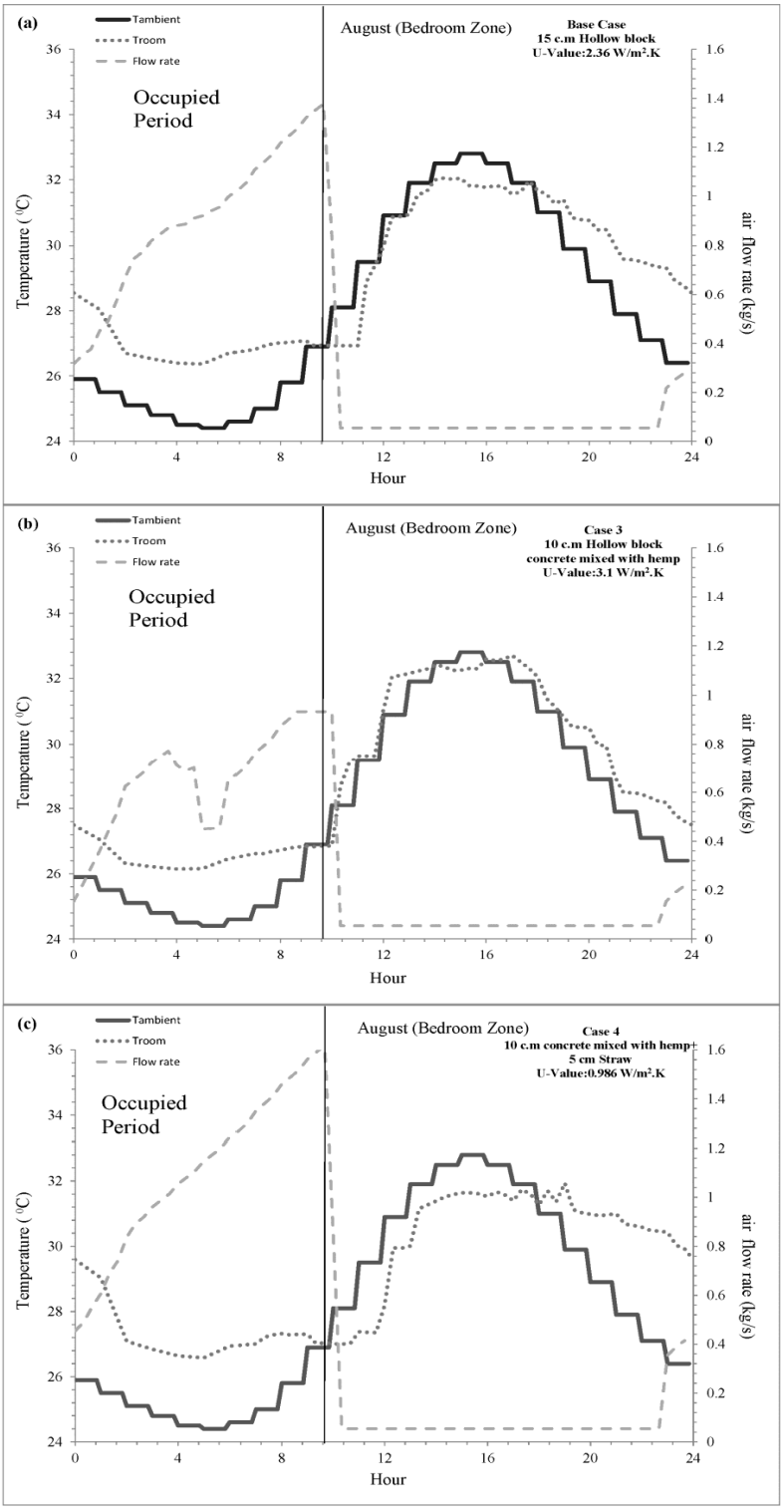
(a)
Tambient
Troom
Flow rate
August (Bedroom Zone)
Base Case
15 c.m Hollow block
U-Value:2.36 W/m².K
Occupied Period
Temperature (°C)
air flow rate (kg/s)
Hour
(b)
Tambient
Troom
Flow rate
August (Bedroom Zone)
Case 3
10 c.m Hollow block concrete mixed with hemp
U-Value:3.1 W/m².K
Occupied Period
Temperature (°C)
air flow rate (kg/s)
Hour
(c)
Tambient
Troom
Flow rate
August (Bedroom Zone)
Case 4
10 c.m concrete mixed with hemp+ 5 cm Straw
U-Value:0.986 W/m².K
Occupied Period
Temperature (°C)
air flow rate (kg/s)
Hour

Fig. 14: Temperature and mass flow rate inside the bedroom zone during August for (a) base case, (b) Case 3, and (c) Case 4.

The numerical model was run for the six simulations (three for each of the living and bedroom zones) for the representative day of each month of the year. The results were multiplied by the number of days in each month to determine the monthly number of discomfort hours in each zone as shown in Fig. 15 (a-b), and the monthly fan consumption as shown in Fig. 16(a-b) for the different scenarios.

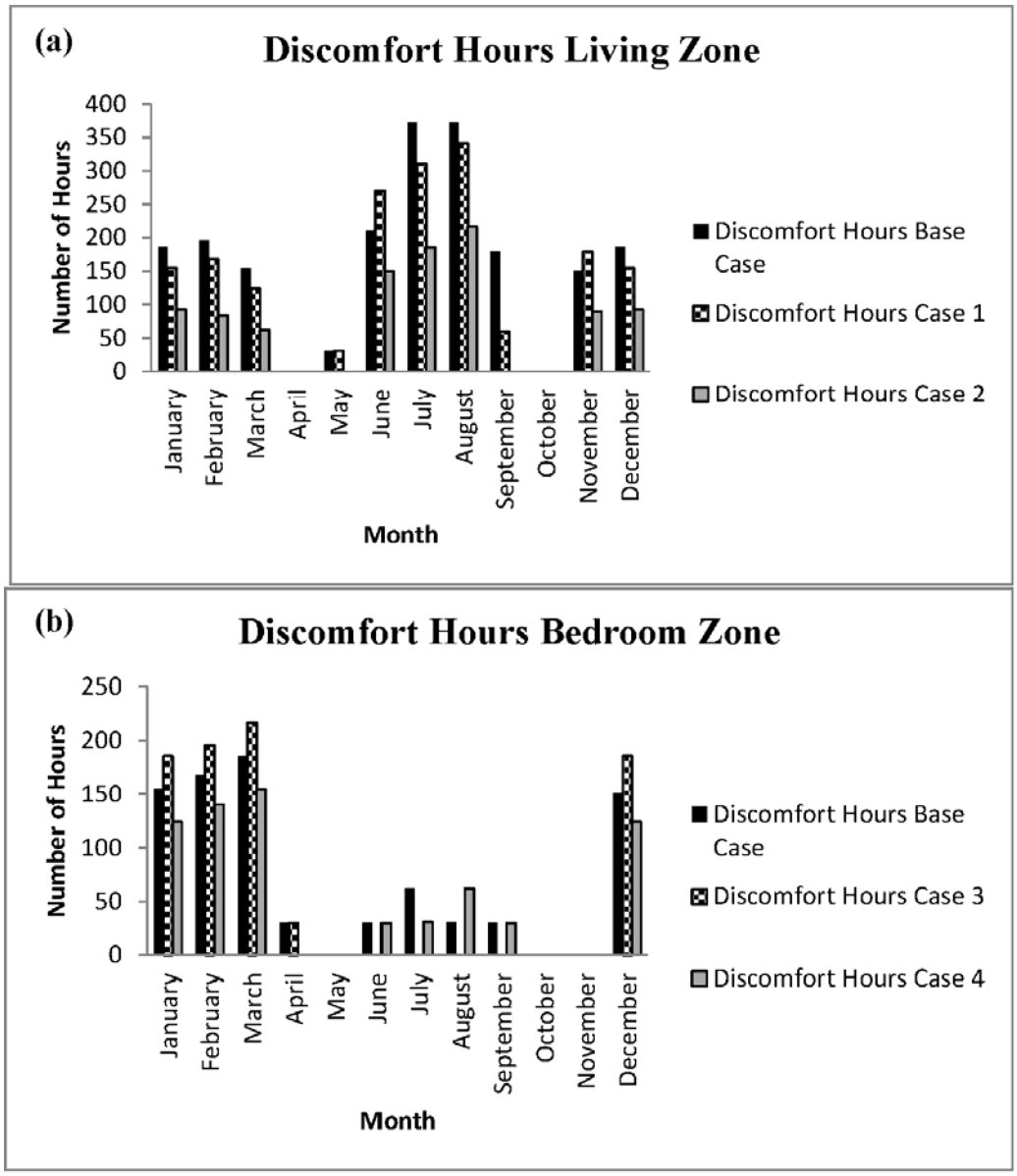

Fig. 15: Number of Discomfort hours for the different cases for (a) living zone and (b) bedroom zone.

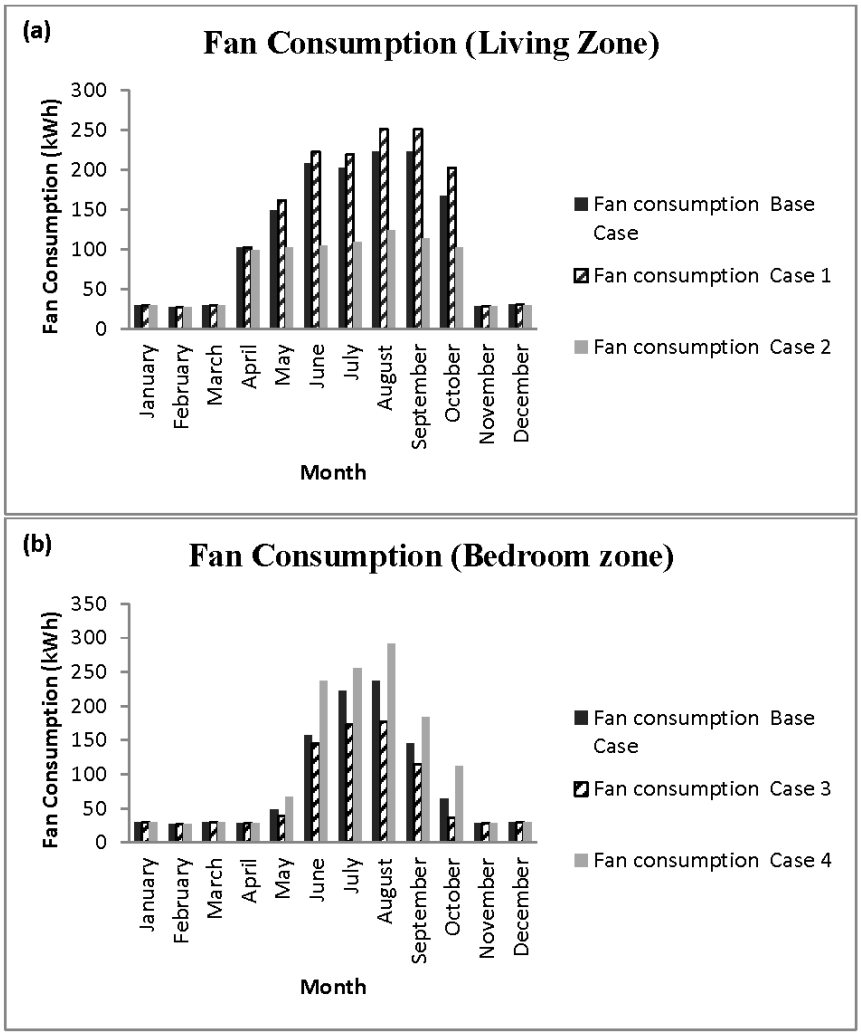

Fig. 16: Fan consumption for the different cases for (a) living zone and (b) bedroom zone.

As shown in Fig. 15 and 16, Case 2 (massive wall in the living zone) has the lowest operational energy and lowest number of discomfort hours during the whole year as compared to the other living zone wall cases. As for the bedroom zone, the base case and Case 3 have approximately equal number of yearly discomfort hours (842 discomfort hour in the base case, and 815 in Case 3); however, even though the high thermal wall insulation, Case 4, has the lowest number of discomfort hours (696

discomfort hour) but it turns to be an in-effective solution for the bedroom since it has a 25.9% increase in the fan energy consumption. On the other hand, bedroom wall Case 3, compared to the base case, can decrease the fan energy consumption by 18.6% and decrease the discomfort hours by 3.2%. However, the discomfort hours mainly occur in the winter during hours when occupants are expected to be sleeping.

From Table 2, it is clear that the use of a mechanical ventilation system for the base case can save around 40.5% of operational energy consumption of the conventional air conditioning system while having 2,880 discomfort hours, 32.8% of discomfort hours during the year. The energy consumption can be reduced by 26.9% and the discomfort hours can be reduced by 37.8% when using wall configuration of Case 2 in the living zone and wall configuration of Case 3 in the bedroom zone.

Table 2: Mechanical ventilation electrical consumption and number of yearly discomfort Hours for the different cases

Configuration wall Case	Yearly Electrical Consumption (kWh/m^2)	Number of yearly discomfort Hours
Base Case (mechanical heating and cooling)	53.53	Not Applicable
Base Case (mechanical Ventilation)(Living + Bedroom)	31.80	2880
Living zone base case	14.32	2038
Living zone Case 1	15.57	1794
Living zone Case 2	9.02	975
Bed room zone base case	17.48	842
Bed room zone Case 3	14.22	815
Bed room zone Case 4	22.01	696

5.3. Results for the rural areas

Figures 17 to 20 present the indoor air temperature for the different wall configurations for the case of mechanical ventilation only, for the months of (a) February, and (b) August, representative months for the winter, and summer seasons. The fan power consumption is calculated based on the affinity law for prime movers. The fan power is proportional to the cube of the flow rate ratio taken with respect to a reference.

During the month of February, since the outdoor air temperature is lower than the indoor air temperature, and the indoor air temperature is less than the set point temperature of 22^{o}C, the ventilation controller set the flow rate to be at its minimal value of 0.054 kg/s throughout the whole simulation day resulting in a fan consumption of 0.96 kWh for all the different configuration in both the living and bedroom zone. Figure 17 (a-c) represents the indoor temperature inside the space for the living zone. The wall configuration 3 (Fig. 17(c)) characterized by high thermal capacitance shows an indoor air temperature profile that tends to store the temperature inside the space during occupancy period. While the reference case (Fig.17 (a)) characterized by lower thermal capacitance shows an indoor air temperature profile that respond to the outdoor temperature variation much more than the other two configurations resulting in 6 discomfort hours occurring during the hours (8 to 10 and 0 19 to 23) as compared to 4 discomfort hours for Wall 1 taking place during the hours (8 to 11 and 22 to 23) and 3 discomfort hours for Wall 2 happening in the morning during the hours (8 to 11).

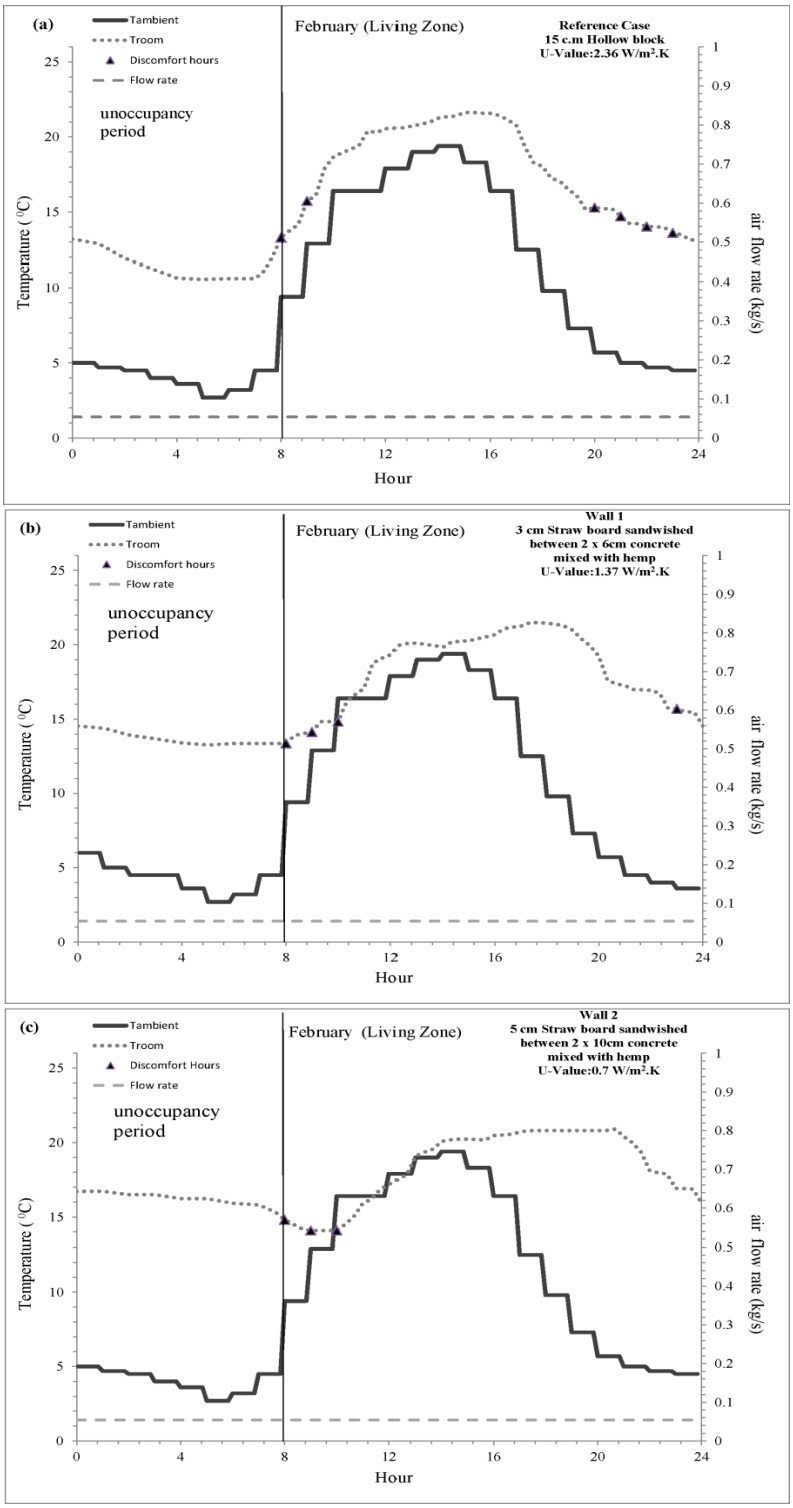

Fig. 17: Temperature and mass flow rate in the living zone during February for (a) reference case, (b) Wall 1, and (c) Wall 2.

In the bedroom zone, due to a higher amount of heat loss between the indoor and the outdoor spaces, wall 4 (Fig. 18(c)) seems to have better conditions in the winter season since it has a 10 discomfort hours between hour (23 till 7) as compared to 11 in the reference case (23 till 8) and 12 in the Wall 3(23 till 9). Moreover, the wall with lowest insulation, Wall 3, Fig. 18(b) corresponds to the lowest air temperature as shown in Fig. 18(b).

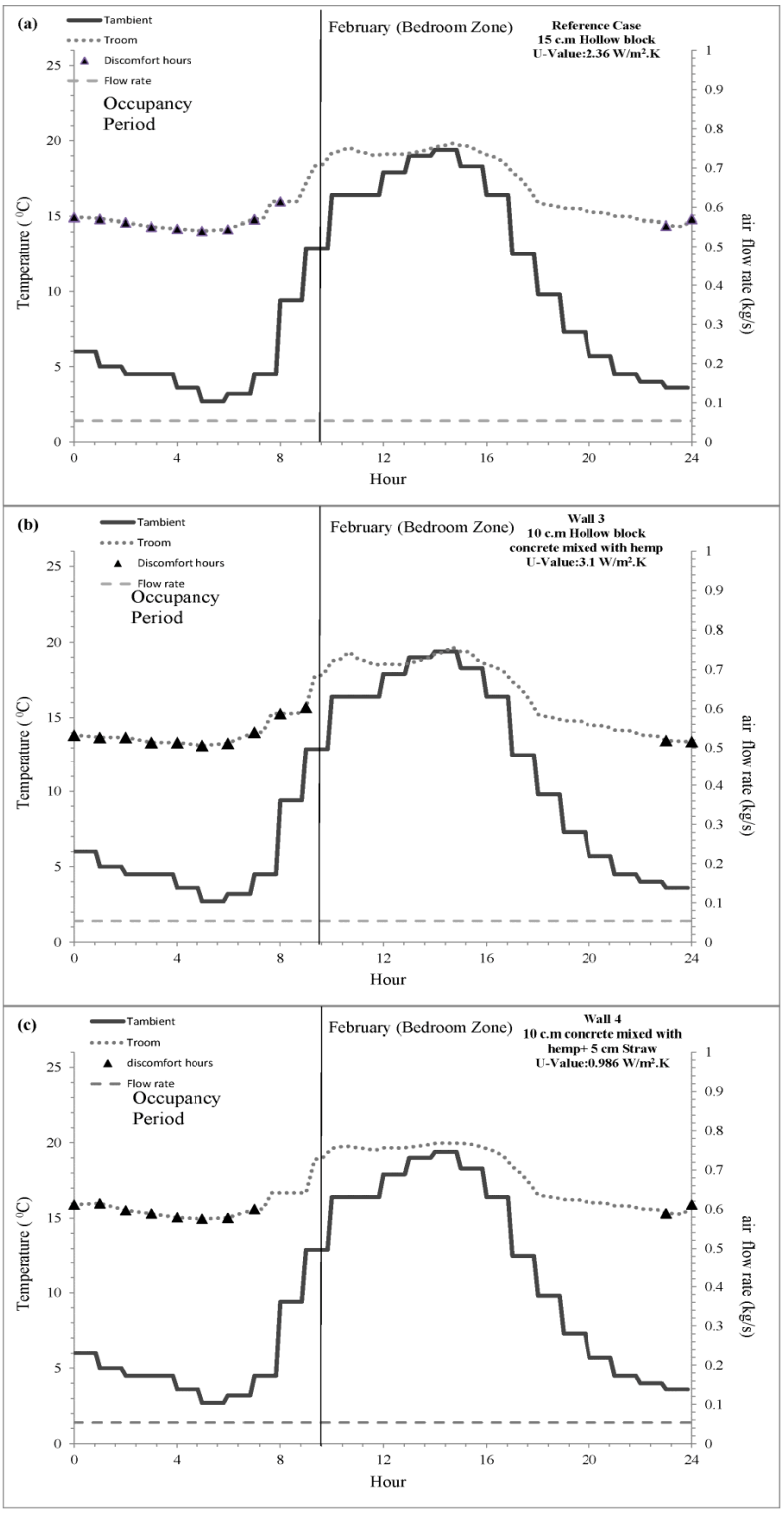

Fig. 18: Temperature and mass flow rate in the bedroom zone during February for (a) reference case, (b) Wall 3, and (c) Wall 4.

As for the month of August, night purging is applied in the living zone, during the day the controller modulated the amount of flow rate brought to the space to prevent the indoor air temperature from increasing beyond the outdoor air temperature. The reference case Fig.19 (a) showed a higher indoor air temperature than Wall 3 (Fig. 19(c)). During the time period 8 to 11, Wall 1 and Wall 2 (Fig. 19 (b) and (c)) showed a lower indoor air temperature than in the reference case. However, in order to enhance thermal comfort inside the space a ceiling fan was turned on inside the space for the period hour extending from 12-19. With the ceiling fan turned on the three different configurations, the number of discomfort hours inside wall 3 (Fig.19 (c) configurations is equal to 8 occurring during the time period (12 to 19) as compared to 11 discomfort hours for the reference case happening during the time period (10 till 20) and 10 discomfort hours for Wall 1 taking place between hour (11 and 20).

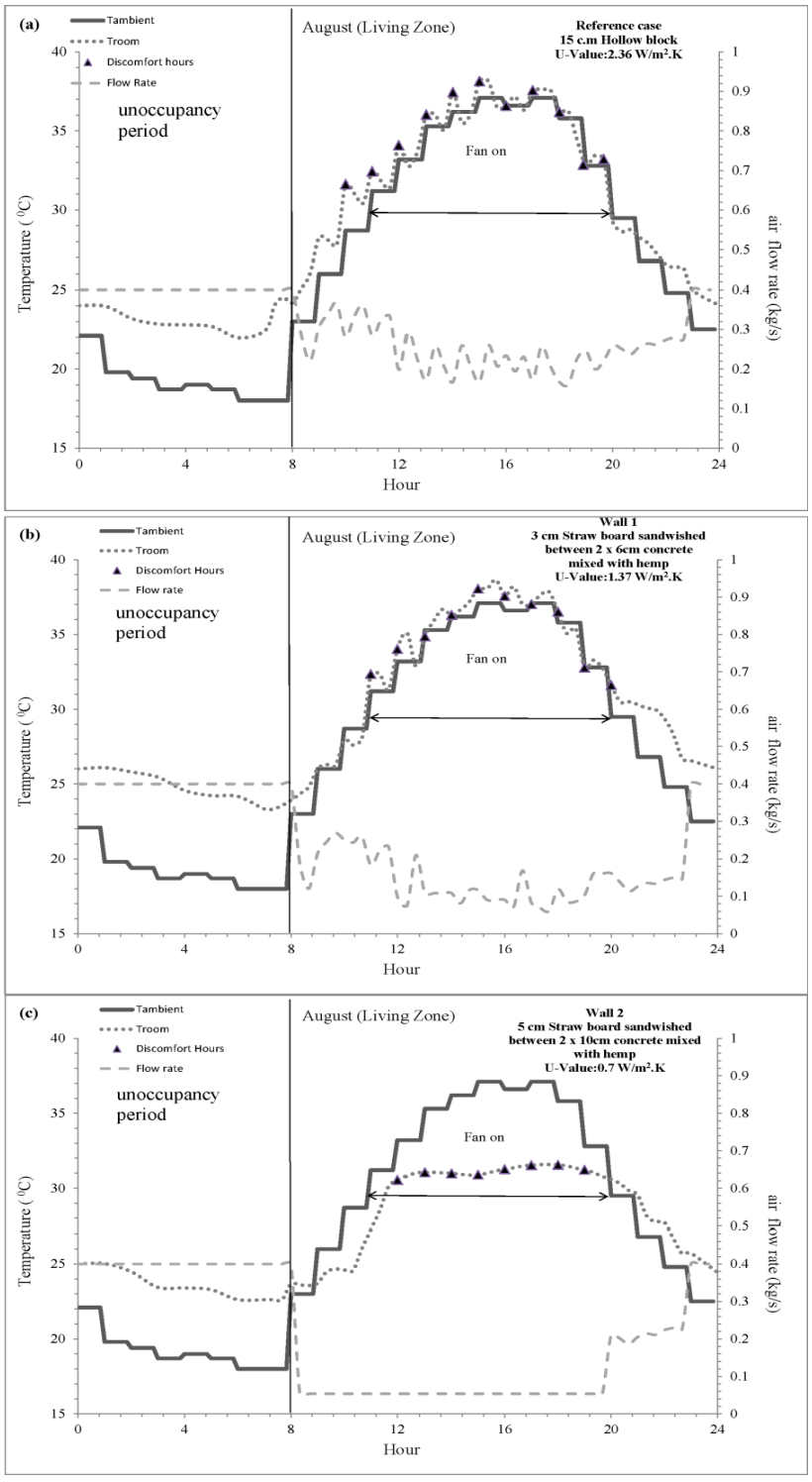

Fig. 19: Temperature and mass flow rate in the living zone during August for (a) reference case, (b) Wall 1, and (c) Wall 2.

In the bedroom zone, Wall 4 (Fig. 9(b)), which is characterized by the lowest heat transfer coefficient, had the highest indoor air temperature at the early hours of the occupied period as compared to the bedroom air temperature of the reference case (Fig. 9(a)) and Wall 3 (Fig. 9(b)). Nonetheless, thermal comfort was attained inside the space during occupancy with zero discomfort hours for the three different wall configurations. moreover due to the lower wall insulation of Wall 3, less ventilation air is needed to moderate the indoor zone temperature (2.25 kWh) as compared to the reference case (2.67 kWh) and (3.22 kWh) for Wall 4.

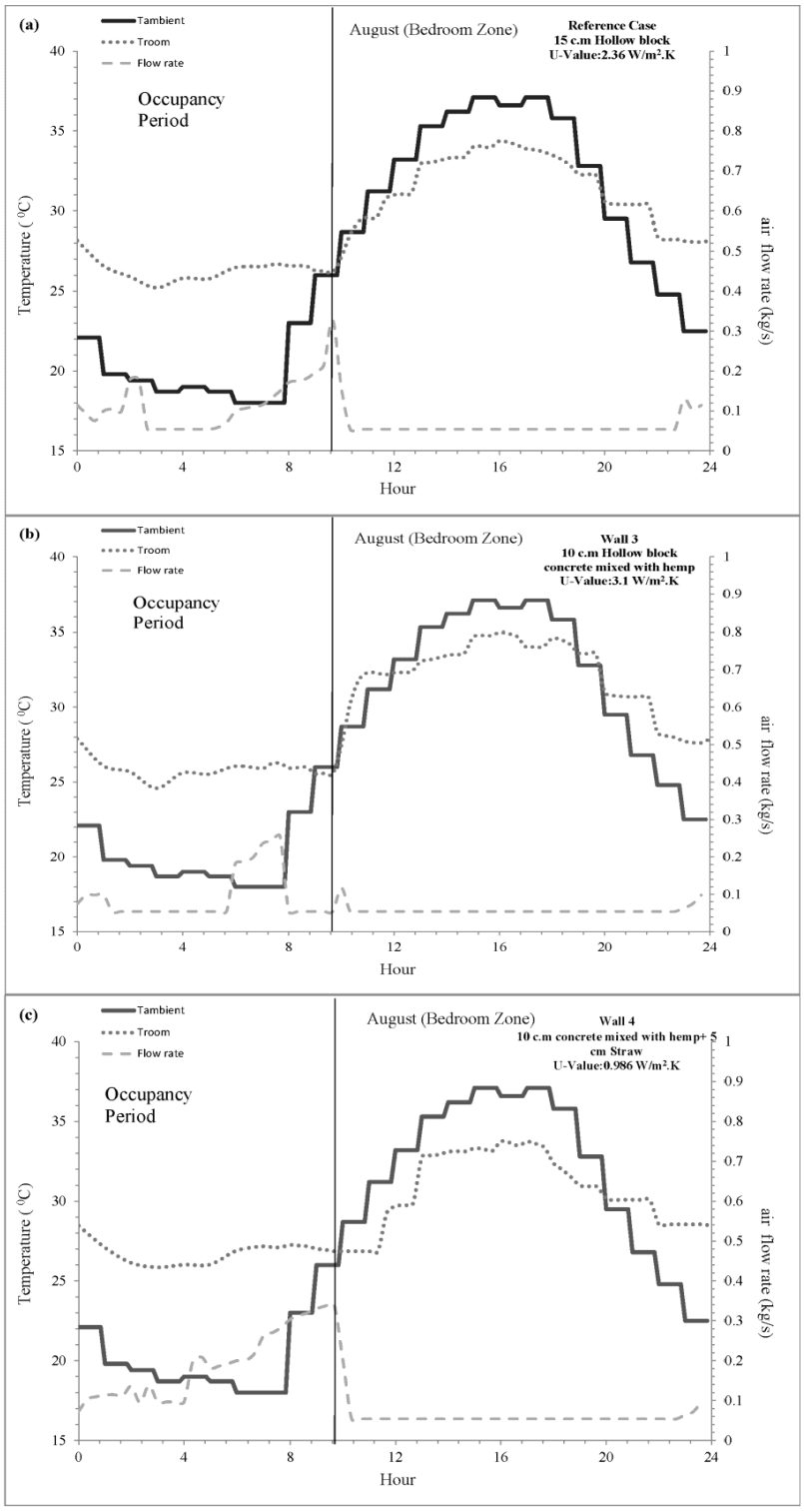

Fig. 20: Temperature and mass flow rate in the bedroom zone during August for (a) reference case, (b) Wall 3, and (c) Wall 4.

The numerical model was run for the seventy two simulations for the representative day of each month of the year. The monthly data are acquired by multiplying the results of the simulation by the number of days in each month. Table 3 represents the number of discomfort hour in the living and bedroom zone while Table 4, represents the monthly fan consumption of the system.

Table 3: Number of Discomfort hours for the different cases for living zone and bedroom zone.

Month	Monthly Discomfort Hours in the living zone		
	reference Case	Wall 1	Wall 2
January	155	124	93
February	168	112	84
March	93	62	31
April	30	0	0
May	0	0	0
June	180	150	120
July	310	279	217
August	341	310	248
September	180	150	120
October	0	0	0
November	0	0	0
December	248	217	186
Month	Monthly Discomfort Hours in the bedroom zone		
	reference Case	Wall 3	Wall 4
January	341	372	310
February	308	336	280
March	310	372	279
April	240	270	180
May	186	217	155
June	90	120	60
July	0	0	0
August	0	0	0
September	0	0	0
October	31	62	0
November	210	240	180
December	372	372	310

Table 4: Number of Discomfort hours for the different cases for living zone and bedroom zone.

Month	Monthly Fan consumption in the living zone		
	reference Case	Wall 1	Wall 2
January	29.76	29.76	29.76
February	26.88	26.88	26.88
March	29.76	29.76	29.76
April	28.8	28.8	28.8
May	29.76	29.76	29.76
June	120.69	136.2	105.3
July	124.496	154.07	112.22
August	132.99	171.43	117.49
September	177.9	188.1	105.3
October	29.76	29.76	29.76
November	28.8	28.8	28.8
December	29.76	29.76	29.76
Month	Monthly Fan consumption in the bedroom zone		
	reference Case	Wall 3	Wall 4
January	29.76	29.76	29.76
February	26.88	26.88	26.88
March	29.76	29.76	29.76
April	28.8	28.8	28.8
May	29.76	29.76	29.76
June	54	50.1	66.3
July	72.23	68.82	89.9
August	82.77	69.75	99.82
September	45.6	43.8	60.6
October	29.76	29.76	29.76
November	28.8	28.8	28.8
December	29.76	29.76	29.76

As shown in table 3 and 4, Wall 2 has the lowest operational energy and lowest number of discomfort hours during the whole year as compared to the other living zone wall configurations. As for the bedroom zone, Wall 4 has the lowest number of

discomfort hour inside the space with 1829 hour compared to 2139 in the reference case and 2418 in Wall 3. Even though the high thermal wall insulation, Wall 4, has an increase of 12.72% in the fan consumption compared to the reference case, but due to the low temperature profile during night of the long winter season in Bekaa region, Wall 4 is considered as the best wall configuration for the bedroom zone.

Since thermal comfort cannot be achieved using the direct ventilation alone, the simulation were run for Wall 2 in the living zone using EAHX during the activation time (Fig.21). Figure 21 that an earth tube of a length of 10 m leads to 12 discomfort hours occurring between hour (9 and 21) with a fan consumption of 15.2 kWh (Fig.10 (a)). Figure 6 (b) represents the temperature and flow rate inside the space for an earth tube of 30 m length, this configuration leads to 6 discomfort hour occurring during hour (12-18) with a fan consumption equal to 14.72 kWh. A 50 m length earth tube lead to 2 discomfort hours (14-16) inside the space, with fan consumption equal to 11.87 kWh (Fig 6(c)).

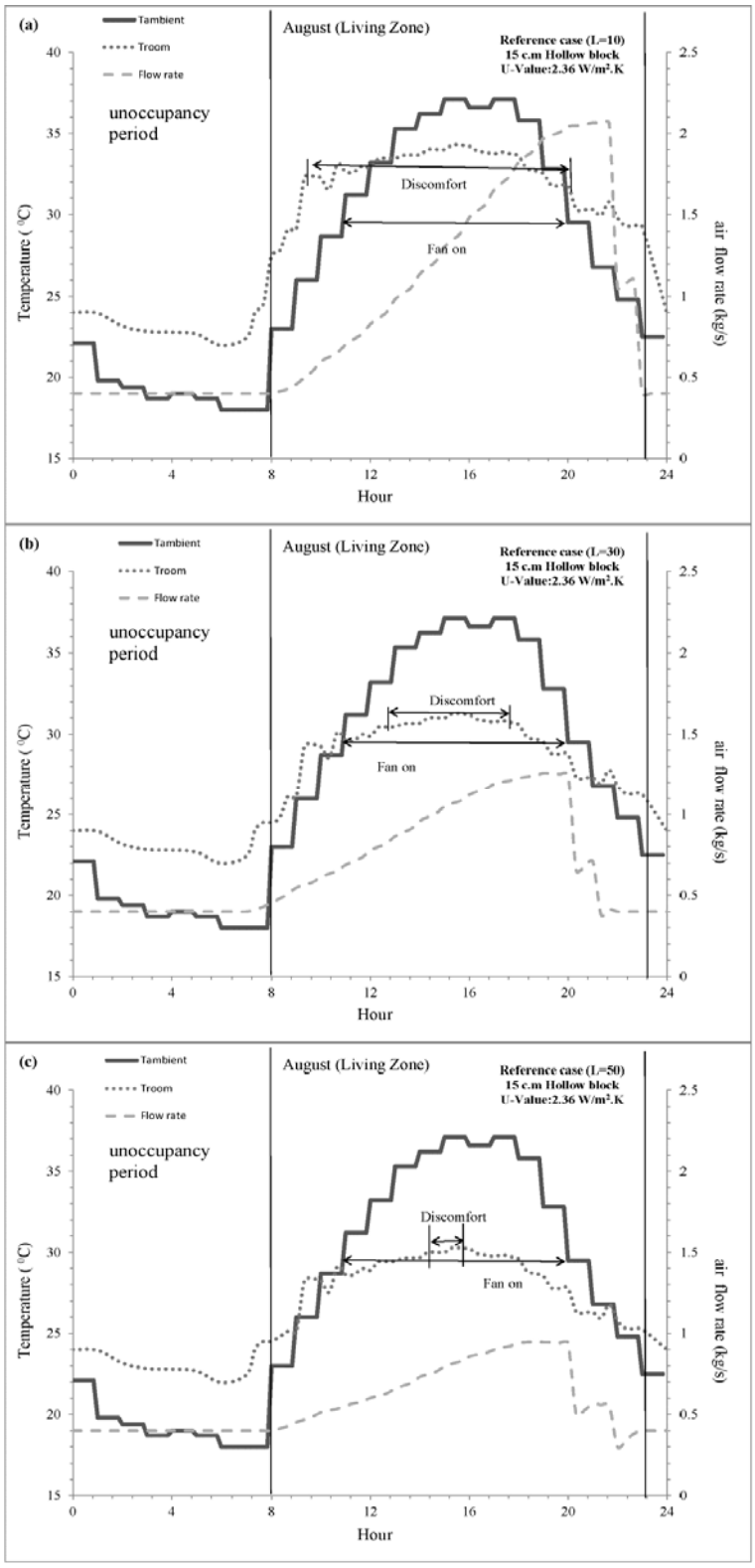

Fig. 21: Temperature inside the space for the different EAHX length configuration

The required pressure to overcome this frictional loss is calculated based on Darcy Weisbach formula, resulting in a required pressure of 297 pa for the 50 m length, 292 pa for the 30 m length and 287 pa for the 10 m length. Thus hybrid mechanical ventilation that can draw air directly from the outside or through the buried pipe is used to bring thermal comfort inside the space with the lowest possible cost. The earth tube placed at 3 m, having a diameter of 0.78 m and a length of 30 m is selected. Thus hybrid mechanical ventilation that can draw air directly from the outside or through the buried pipe is used to bring thermal comfort inside the space with the lowest possible cost. The earth tube placed at 3 m, having a diameter of 0.78 m and a length of 30 m is selected. The simulations are repeated for a configuration of high thermal capacity wall in the Living zone (Wall 2) and a high insulation wall in the bedroom zone (Wall 4).

Figure 22 and 23 represent the temperature inside the space when the EAHX is used during the months of February and August. In February, when the indoor temperature inside the space becomes lower than 16^{o}C during the time period (8 till 11), Air is allowed to pass through EAHX; the temperature inside the space tends to increase by 1^{o}C when compared to the case where EAHX was disabled. The discomfort hours has been reduced by 1 hour, resulting in two discomfort hours (Fig.22).

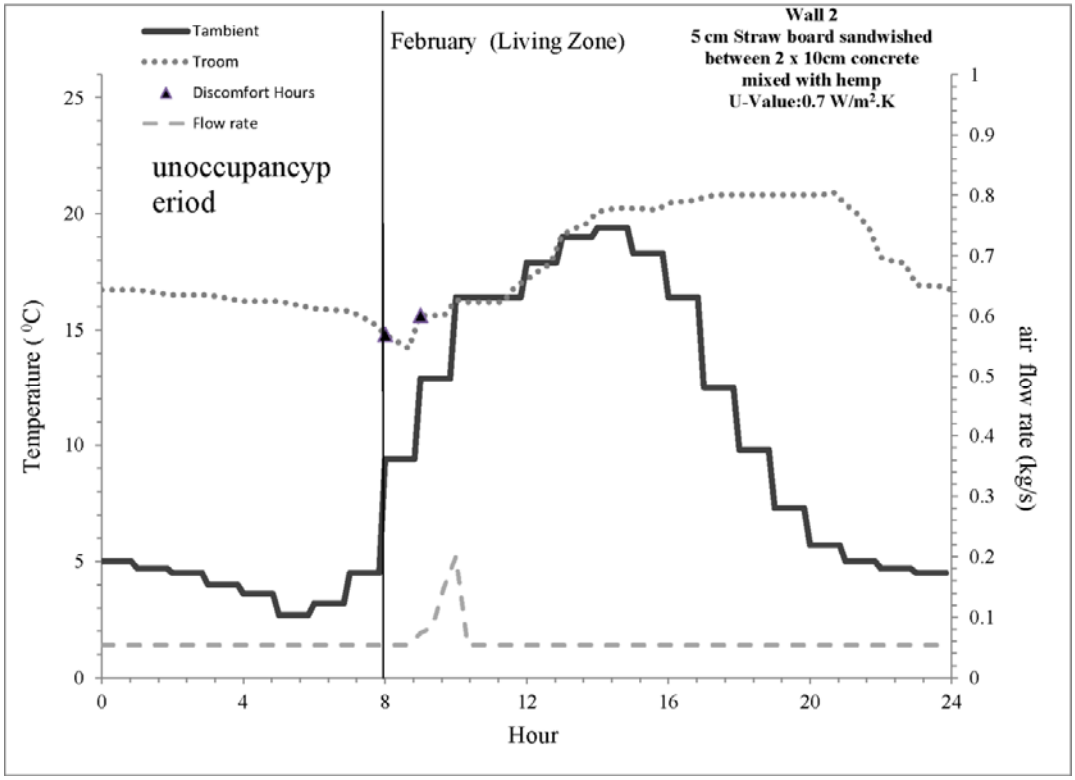

Fig. 22: Temperature inside the living zone with the EAHX activated during the month of February.

During August, when the indoor temperature becomes higher than 30^{o}C (at 11), the EAHX is activated; air is allowed to pass through the buried pipe. At hour 20, the EAHX was set to the deactivation mode since the temperature inside the space becomes equal to the set point temperature. At hour 21, the outside temperature becomes less than the set point temperature, thus the direct ventilation system is activated again. During the time period, when the EAHX is active 1 discomfort hour has occurred compared to 8 discomfort hours when the EAHX is not used. However, the fan consumption has increased to 12.6 kWh (3.2 kWh during the direct ventilation and 9.4 kWh during the EAHX).

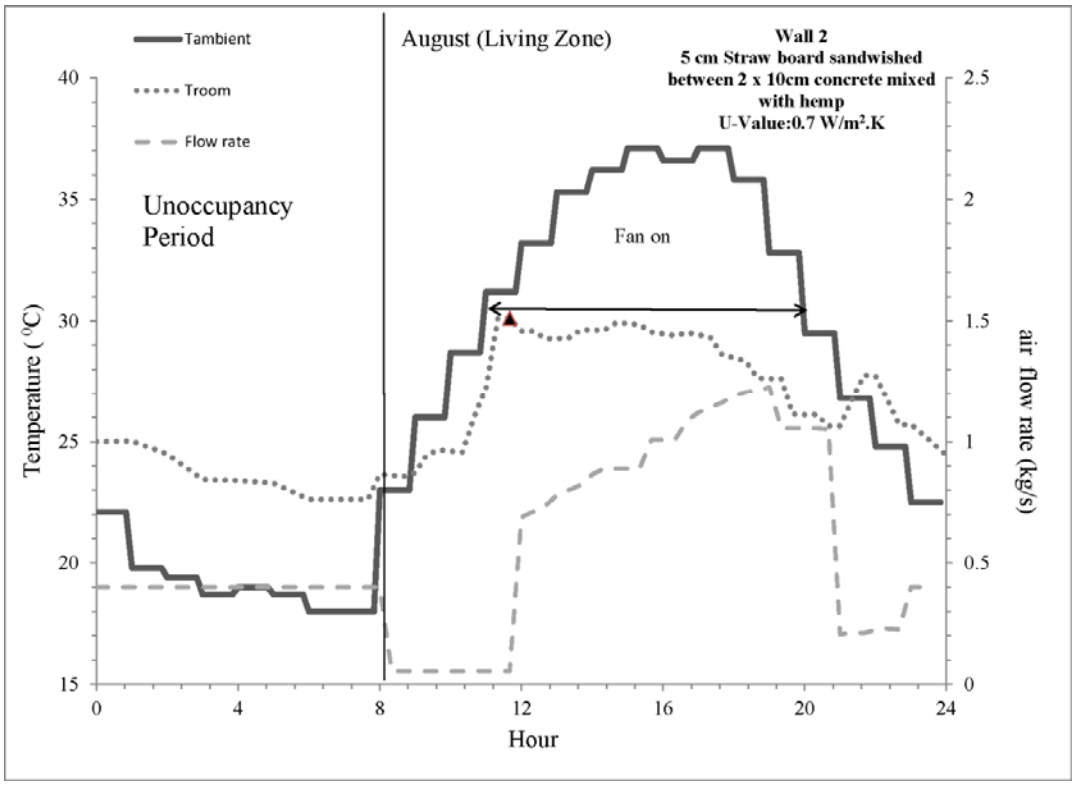

Fig. 23: Temperature inside the living zone with the EAHX activated during the month of August.

Table 5 represents the yearly electrical consumption and the yearly discomfort hours. By relying on mechanical ventilation instead of Mechanical cooling and heating system a 73% in electrical consumption can be saved, even though of this saving the discomfort hours in the reference case constitutes 43.29% of the total hours of the years. Thus, as said earlier Wall 2 in the living zone has the lowest operational energy with a decrease in the power consumption by 14.70% while having a decrease in the number of discomfort hour by 35.54% compared to the reference case. On the other hand, by using an EAHX in the living zone combination (Wall 2 in the living zone), the number of discomfort hours in the apartment can decrease by 72% compared to the Wall 2 without EAHX and a decrease by 82% compared to the reference case without EAHX. However

the fan power consumption has increased by 46% compared to the Wall 2 without EAHX and with an increase 36% compared to the reference case (Table 6).

Table 5: Mechanical ventilation electrical consumption and number of yearly discomfort Hours for the different cases

Configuration wall Case	Yearly Electrical Consumption (kWh/m^2)	Number of yearly discomfort Hours
Reference case (mechanical heating and cooling)	60.04	0
Reference case (mechanical Ventilation)(Living + Bedroom)	16.02	3793
Living zone reference case	7.89	1705
Living zone Wall 1	8.83	1404
Living zone Wall 2	6.73	1099
Bed room zone reference case	8.13	2088
Bed room zone Wall 3	7.76	2361
Bed room zone Wall 4	9.16	1754

Table 6: Mechanical ventilation electrical consumption and number of yearly discomfort Hours for the living with and without earth to air heat exchanger (EAHX)

	Yearly Discomfort hours	Yearly Electrical Consumption (kW/m^2)
Living zone without EAHX	1099	6.73
Living Zone With EAHX	304	12.47

CHAPTER 6

CONCLUSION

This thesis integrates space and comfort and ventilation controller models into one model. Through simulation, the integrated model determines the amount of ventilation air that can possibly provide indoor thermal comfort for longer periods. This allows for accurately measuring the energy performance of buildings and assessing the operational energy of various building envelop designs.

In order to validate the simulation results, a typical house in Beirut, Lebanon, is modeled in TRNSYS (TRNSYS 2006). This required calibrating TRNSYS against published data, and then comparing the results against the proposed numerical model. The analysis confirmed that the building design parameters affect the thermal comfort inside the space and fan consumption of the mechanical ventilation system. The simulation results revealed that a combination of a massive wall made of a 5 cm layer of straw sandwiched between 2× 10 cm of Hempcrete in the living zone, and in addition to 10 cm of Hempcrete in the bedroom zone, can reduce the operational cost of the house by 26.9% and the discomfort hours by 37.8% compared to the base case.

In the inland region, the simulations are done in three phase approaches. In the first phase, the analysis confirmed that in case of hot summer and cold winter, Natural and Mechanical ventilation cannot assure thermal comfort inside the space however integration between mechanical ventilation and an earth tube heat exchanger model can decrease the number of discomfort hours. The simulation results revealed that a combination of a massive wall made of a 5 cm layer of straw sandwiched between 2×

10 cm of Hempcrete in the living zone, and in addition to 10 cm of Hempcrete with 5 cm of insulation in the bedroom zone were the best wall configuration for the case of direct ventilation. The simulation revealed that those configurations can reduce the operational cost of the house by 0.77% and the discomfort hours by 24.78% compared to the reference case. In the second phase, the length of the earth tube that can minimize the discomfort hours was investigated. In the third phase, the run were carried out for the best wall configuration determined in the first approach with the hybrid mechanical ventilation. When the earth tube heat exchanger is used the number of discomfort hour has been reduced to 23.49% of discomfort hours during the whole year which is a decrease by 45.74% compared to the reference case with direct ventilation. However, the fan power consumption has increased by 25.94% compared to the best configuration (Wall 2 in the living zone and Wall 4 in the bedroom zone) with direct ventilation.

REFERENCES

ASHRAE Standard 55 1992.Thermal Environmental Conditions for Human Occupancy, ASHRAE, Atlanta.

Climate, Comfort, & Natural Ventilation: A new adaptive comfort standard for ASHRAE Standard 55 2001, University of California, Berkeley.

Givoni, B., 2011. Indoor temperature reduction by passive cooling systems. Solar Energy 85 (8), 1692-1726.

Yassine, B., 2012. A numerical modeling approach to evaluate energy-efficient mechanical ventilation strategies in urban and rural areas, Master Thesis, American university of Beirut.

Jacovides, C.P. , Mihalakakou, G., 1995. An underground pipe system as an energy source for cooling/heating purposes, Renewable Energy 6 (8), 893-900.

Derbel, H. Ben Jmaa, Kanoun, O., 2010. Investigation of ground thermal potential in Tunisia focused towards heating and cooling applications, Thermal engineering (30), 1091-1100.

Dhaliwal AS, Goswami, DY., 1984. Heat transfer analysis environment control using an underground air tunnel. ASME Solar EnergyDiv. LasVegas ,, 505–10.

Dorf, R., R. Bishop, 2008. Modern Control Systems 11th edition, Person International Edition, Person Education.

Awwad E., Hamad B., Mabsout M., Khatib H., 2010. Sustainable Construction Material Using Hemp Fibers – Preliminary Study, Second International conference on sustainable construction Materials.

Shaviv, E., Yezioro, A., Capeluto I. G., 2001.Thermal Mass and Night Ventilation as Passive Cooling Design Strategy. Renewable Energy 24 (3-4), 445-452.

Alajmi, F., Loveday, D. and Hanby, V., 2006. The cooling potential of earth–air heat exchangers for domestic buildings in a desert climate, Building and Environment 41 (3), 235-244.

Ascione, F., Bellia, L., and Minichiello F., 2011. Earth-to-air heat exchangers for Italian climates, Renewable Energy 36 (8),2177-2188.

Fanger, P. O. 1970. Thermal Comfort. Copenhagen: Danish Technical Press.

Carrilho da Graca, G., Chen, Q., Glicksman, L.R., Norford, L.K., 2002. Simulation of wind driven ventilative cooling systems for an apartment building in Beijing and Shanghai. Energy and Buildings 34, 1–11.

Mihalakakou, G., Santamouris, M., Asimakopoulos, D., Tselepidaki. D., 1995. Parametric prediction of the buried pipes cooling potential for passive cooling applications. Solar Energy 55 (3), 163–73.

Zhou, J., Zhang, G., Lin, Y., Li, Y., 2008. Coupling of thermal mass and natural ventilation in buildings. Energy and Building 40, 979–986.

Lee, K., and Strand, R., 2008. The cooling and heating potential of an earth tube system in buildings. Energy and Buildings 40, 486-494.

Labs, 1989. In: J. Cook (Ed.), Passive Cooling, MIT Press, Cambridge, Massachusetts.

Kolokotroni, M., Aronis, A., 1999. Cooling-energy reduction in air-conditioned offices by using night ventilation. Applied Energy 63 (4), 241-253.

Krarti, M., 1995. Analytical Model to predict annual soil surface temperature Variation, Journal of solar engineering 117 (2), 91-99.

Meteonorm, www.meteonorm.com

Ghaddar, N., Bsat, A., 1998. Energy conservation of residential buildings in Beirut. International Journal of Energy Research, 22, 523–546.12

Blondeau, P., Spérandio, M., Allard, F., 1997. Night ventilation for building cooling in summer. Solar Energy 61 (5), 327-335.

Hollmuller, P., and Lachal, B., 2001. Cooling and preheating with buried pipe systems: monitoring, simulation and economic aspects 33,509-518.

Republic of Lebanon Ministry of Public Works and Transport. Energy Analysis and Economic Feasibility. UNDP/GEF, MPWT/DGU, 2005, 63.

Elfordy, S., Lucas F., and Tancret, F., 2008. Mechanical and thermal properties of lime and hemp concrete (‘“hempcrete”’) manufactured by a projection process, Construction and Building Materials 22, 2116-2123.

Shingari, BK., 1995. Earth tube heat exchanger. Poultry International 34 (PT 14):92–7.

Kusuda, T., Achenbach, P.R., 1965. Earth Temperature and Thermal diffusivity on at Selected Stations in the United States, ASHRAE Trans. 71,61–75.

The Green Building Bible. 3rd edition Volume 1 & 2. Publishing editor Keith Hall (Contributory authors specified when relevant) Published by The Green Building Press. ISNB 1-898130-03-05 (volume 1), 1-898130-04-3 (volume 2).

Thermo hemp Technical Data Sheet, ecological building systems, Stand, 2007, 758026-758026, www.ecologicalbuildingsystems.com

TRNSYS, Transient System Simulation Tool Software. **Thermal Energy System Specialists, LLC.** Madison Wisconsin. http://www.tess-inc.com/**,** accessed on 25-June-2012.

U. Eicker, Cooling strategies, summer comfort and energy performance of a rehabilitated passive standard office building. Applied Energy 87 (6) (2010) 2031-2039.

United Nation Development Program, Lebanon Page, **http://www.undp.org.lb/programme/pro-poor/poverty/povertyinlebanon/conditions97.cfm**, accessed on 17-June-2012.

Bansal, V., Misra, R., Agrawal, G.D., and Mathur, J., 2010. Performance analysis of earth–pipe–air heat exchanger for summer cooling, Energy and Buildings 42 (5), 645-648.

Geros, V., Santamouris, M., Tsangrasoulis, A., Gurracino, G., 1999. Experimental Evaluation of night ventilation phenomena. Energy and buildings 29, 141-154.